

N 70 15678

SU-SEL-69-019

NASA CR 107653

# Magnetic Radiation Observed by the OGO-1 and OGO-3 Broadband VLF Receivers

by

W. J. Burtis

August 1969

TECHNICAL REPORT NO. 3438-1



Prepared under  
National Aeronautics and Space Administration  
Contract NAS 5-2131  
Grant NGR 05-020-288

## CASE FILE COPY

**RADIOSCIENCE LABORATORY**  
**STANFORD ELECTRONICS LABORATORIES**  
**STANFORD UNIVERSITY • STANFORD, CALIFORNIA**



MAGNETIC RADIATION OBSERVED BY THE OGO-1 AND OGO-3  
BROADBAND VLF RECEIVERS

by  
W. J. Burtis

August 1969

Technical Report No. 3438-1

Prepared under  
National Aeronautics and Space Administration  
Contract NAS 5-2131  
Grant NGR 05-020-288

Radioscience Laboratory  
Stanford University                      Stanford, California



## ABSTRACT

The OGO-1 and OGO-3 broadband VLF (0.3 - 13.0 kHz) receivers observe recurring forms of magnetic radiation in the magnetosphere. On the basis of simple spectral characteristics the most commonly observed radiation may be classified as banded chorus, banded hiss, or low-frequency noise. Banded chorus consists of a band of discrete, narrowband emissions whose center frequency  $f$  is between  $0.1$  and  $0.6 f_{Ho}$ , where  $f_{Ho}$  is the minimum gyrofrequency on the fieldline passing through the satellite. During the latter half of 1966 banded chorus was observed most commonly (on about 50% of the passes) in a region extending from  $L \sim 4 - 5$  near the dawn meridian to  $L \sim 6 - 8$  in the early afternoon. Occurrence seemed to be independent of dipole latitude in the range  $\pm 40^\circ$ , but was positively correlated with magnetic activity. The parallel energy of gyroresonant electrons is estimated to be on the order of 10 keV. A tentative calibration indicates rapid rise times to broadband amplitudes typically on the order of 10 - 100 milligammas during discrete banded chorus emissions. Banded hiss consists of a band of diffuse, unstructured radiation in the same normalized frequency range ( $0.1 < f/f_{Ho} < 0.6$ ) as banded chorus. It was not observed as commonly as the latter but occurred in a roughly similar region. Low-frequency noise consists of radiation at frequencies generally below  $0.1 f_{Ho}$ . It seldom shows discrete structure and usually extends to the 300 Hz low-frequency cutoff of the receiver. It was observed most commonly (on about 70% of the passes) at low L-values, generally within the plasmasphere. On a single occasion narrowband radiation was observed above the expected local electron gyrofrequency.

CONTENTS

	<u>Page</u>
I. INTRODUCTION .....	1
A. VLF Emissions .....	1
B. Contributions of the Present Work .....	4
C. Satellite Orbits and Equipment .....	5
D. Interpretation of Spectrograms .....	6
II. CHARACTERISTICS OF VLF RADIATION IN THE MAGNETOSPHERE .....	8
A. The Data .....	8
B. Banded Chorus .....	18
C. Banded Hiss .....	29
D. Low-Frequency Noise .....	30
E. Comparison of OGO-1 and OGO-3 Data .....	32
F. Amplitude of Banded Chorus .....	33
G. Latitude Dependence .....	37
H. Dependence on Magnetic Activity .....	41
I. An Unusual Observation of Noise above the Gyro- frequency .....	48
III. SUGGESTIONS FOR FURTHER RESEARCH .....	53
REFERENCES .....	55

ILLUSTRATIONS

<u>Figure</u>		<u>Page</u>
1	Satellite orbits for the period for which occurrence statistics were calculated .....	9
2	Examples of banded chorus, showing the confinement of discrete emissions to a single frequency band .....	11
3	Examples of banded hiss, showing the confinement of non-structured activity to a single frequency band somewhere between $0.1$ and $0.6 f_{Ho}$ .....	13
4	Examples of low-frequency noise .....	14
5	Simultaneous data from the broadband receiver and the band 1 and band 2 digital sweeping receivers on OGO 1 .....	16
6	Satellite orbits and activity for one representative 3-hour local time block (2100-2400 LT) .....	19
7	Occurrence statistics for three types of VLF radiation, as a function of $R_o$ and local time .....	20
8	Occurrence of banded chorus as a function of $R_o$ and local time plotted in the equatorial plane .....	22
9	Occurrence of banded chorus as a function of quasi-invariant latitude QINV and local time .....	25
10	Comparison of occurrence of VLF chorus .....	26
11	Examples of the amplitude variation of banded chorus emissions observed by OGO 1 .....	36
12	Occurrence statistics for three types of VLF radiation as a function of dipole latitude $\phi$ for various $R_o$ .....	38
13	The number of observations of banded chorus at various normalized frequencies for dipole latitudes $\phi$ within $10^\circ$ of the equator and for all other dipole latitudes .....	40
14	Occurrence of three types of VLF radiation between 0600 and 0900 local time as a function of $R_o$ , for magnetically quiet and moderately disturbed periods .....	42
15	Examples of banded chorus for varying degrees of magnetic disturbance (higher $K_p$ values at the top) .....	46
16	$D_{st}$ values for a 3-week period in October 1966 .....	47

ILLUSTRATIONS (cont.)

<u>Figure</u>		<u>Page</u>
17	OGO-3 orbit for 10 September 1966, during part of which radiation was observed above the local (Williams-Mead) gyrofrequency $f_H$ .....	49
18	Unusual narrowband radiation above the local (Williams-Mead) electron gyrofrequency .....	50

TABLE CAPTION

<u>Table</u>		<u>Page</u>
1	Banded chorus activity, OGO 1, 06-09 LT .....	45

## ACKNOWLEDGMENT

I express my thanks to Professor Robert A. Helliwell for his enthusiasm and guidance throughout the course of this research. Many helpful discussions with J. J. Angerami, D. L. Carpenter, N. Dunckel, J. P. Katsufakis and other members of the Stanford Radioscience Laboratory are gratefully acknowledged. Dr. G. D. Mead kindly provided a computer subroutine for calculating the locus of the magnetic fieldline passing through the satellite; these calculations were carried out by N. Dunckel.

This research was supported by the National Aeronautics and Space Administration under contract NAS 5-2131 and grant NGR 05-020-288.



## I. INTRODUCTION

### A. VLF EMISSIONS

Electromagnetic radiation at very low frequencies (VLF,  $f < 30$  kHz) may be divided into two broad categories: whistlers and emissions. Whistlers, which are dispersed impulses generated by lightning, have been extensively studied and continue to yield valuable information on the plasma environment of the earth. Emissions, broadly defined, include all other naturally occurring VLF radiation, most of which is thought to be generated by elementary particles in or above the ionosphere. Emissions occur with wide variations of frequency, intensity, and spectral form.

Prior to 1959 all VLF observations were made below the ionosphere. Gallet [1959] classified emissions as "continuous" or "discrete" in frequency. The former is often called "hiss", while a composite of many discrete emissions is called "chorus". Pope [1963] found that the diurnal maximum of chorus occurred later at higher latitude stations, and that the maximum chorus frequency was higher at night than during the day. Laaspere et al. [1964] reported that the center frequency of chorus generally decreased with increasing latitude. Helliwell [1965] reviewed the state of knowledge of emissions and prepared an extensive atlas illustrating spectrograms of typical ground station observations.

Ground observations are limited to that portion of VLF radiation which is at the right frequency and angle of incidence and of sufficient intensity to penetrate the ionosphere. Early, low altitude satellites carrying VLF receivers, including Injun 3 [Gurnett and O'Brien, 1964] and Alouette 1 [Barrington et al., 1963], confirmed the existence of stronger VLF radiation above the ionosphere and observed new types of emissions not seen on the ground. Even at these altitudes, however,

radiation propagating down from the magnetosphere may be reflected above the satellite, and the ray paths followed by the observed signals are uncertain due to the complicated and variable composition of the topside ionosphere.

OGO 1, launched in 1964, carried the first VLF receiver into the outer magnetosphere. Using the digital stepping receivers, Dunckel and Helliwell [1969] described the occurrence and intensity of emissions below the electron gyrofrequency. They found that the highest observed frequency was proportional to the equatorial gyrofrequency on the field-line passing through the satellite, but that the strongest radiation usually occurred near the receiver low-frequency cutoff of 300 Hz. Ficklin et al. [1969] studied emissions having components above the electron gyrofrequency. The present study is based on observations by the broadband VLF receiver onboard the same satellite and OGO 3. This receiver provides detailed spectral resolution of the emissions.

The source of most VLF emissions is generally assumed to be elementary charged particles spiraling along geomagnetic fieldlines. (Other satellite-observed emissions may be nonpropagating electrostatic oscillations of the ambient plasma). Energetic particles may in general emit cyclotron and Cerenkov radiation; one problem is to account for the observed strength of the emissions, another is to explain the coherent narrowband character of discrete emissions. Electrons emitting cyclotron radiation at a frequency equal to their gyrofrequency Doppler-shifted downward by their streaming velocity were considered by Stepenov and Kitsenko [1961] and Dowden [1962]. The generation mechanism may be viewed as a transverse resonance plasma instability which proceeds spontaneously when the resonant electron population has pitch angle

anisotropy [Bell and Buneman, 1964; Brice, 1964b]. The radiation may phase incoming electrons to produce discrete emissions [Brice, 1963; Helliwell, 1967].

VLF emissions probably play an important part in the dynamics of certain transient electron populations in the magnetosphere connected with geomagnetic storms. This is an active area of research, but the following tentative picture is representative of current ideas. Following a magnetic substorm, enhanced fluxes of keV electrons appear in the morning magnetosphere; these may be previously trapped lower energy particles which have been accelerated, or they may be electrons which have drifted in from the geomagnetic tail or the evening magnetosphere [Jelly and Brice, 1967; Kavanagh et al., 1968]. Some of these may generate VLF emissions through gyroresonance interactions. This cyclotron radiation may in turn decrease the pitch angles of trapped electrons in a random walk process until some electrons finally reach the loss cone and are precipitated [Kennel and Petschek, 1966]. Some of the precipitating electrons may emit bremsstrahlung radiation known as X-ray microbursts [Oliven and Gurnett, 1968].

A more thorough understanding of the properties of VLF emissions is first of all desirable in connection with the above interaction with trapped electrons. The Kennel-Petschek [1966] theory envisioned broadband radiation far below the electron gyrofrequency, whereas much of the observed radiation is in fact discrete and near half the gyrofrequency. At these frequencies electrons will diffuse in energy as well as pitch angle, and the applicability of the theory is unclear. It may be hoped that eventually the quantitative study of discrete emissions will provide a diagnostic tool for measuring the space and velocity

distribution of transient particles. In addition, ambient properties of the tenuous region beyond the plasmapause such as density gradients and magnetic field distortions might be investigated through their effects on the propagation of VLF emissions. The study of natural VLF emissions is valuable in its own right as an investigation of plasma instabilities in an environment which cannot be duplicated in the laboratory.

#### B. CONTRIBUTIONS OF THE PRESENT WORK

The present paper is part of a continuing study of the properties of VLF emissions, using observations from the OGO satellites as well as from ground stations. It is concerned specifically with radiation observed by the broadband VLF receivers onboard OGO 1 and OGO 3, primarily during autumn 1966. Three distinct classes of emissions are defined and illustrated: banded chorus, banded hiss, and low-frequency noise. The occurrence of radiation in each class is investigated as a function of magnetic shell, dipole latitude, local time, and magnetic activity. The relation of this radiation to VLF emissions observed on the ground and in the topside ionosphere is discussed. Energies are calculated for gyroresonant electrons which may generate banded chorus. The amplitude of banded chorus radiation is estimated and rise and fall times of discrete emissions are illustrated.

This study is complementary to that of Dunckel and Helliwell [1969] using the OGO 1 digital VLF stepping receivers. It is also closely related to a previous paper [Burtis and Helliwell, 1969] which interprets some of the properties of banded chorus in terms of generation and propagation of the radiation.

### C. SATELLITE ORBITS AND EQUIPMENT

Satellites OGO 1 and OGO 3 are members of the Eccentric Orbiting Geophysical Observatory series and have highly elliptical, moderate-inclination earth orbits. In September, 1966, during the time of data collection for the present study, the perigee of OGO 1 was about  $3.6 R_e$  (earth radii, geocentric), apogee was about  $22 R_e$ , the inclination was  $52^\circ$ , and the period was 63 hours 58 minutes; the perigee was slowly increasing at a rate of about one earth radius per year. The orbit was such that OGO 1 tended to enter the magnetosphere at high southern latitudes, cross the dipole equator near perigee, and exit the magnetosphere at high northern latitudes. OGO 3 had a much lower perigee of about  $1.10 R_e$ , apogee  $20 R_e$ , inclination  $34^\circ$ , and period 48 hours 33 minutes. During its inbound passage through the magnetosphere OGO 3 tended to remain at low latitudes near the dipole equator, while during its outbound passage (some 7 hours earlier in local time) it tended to be at northern midlatitudes. Each satellite remained within the magnetosphere for several hours each pass.

Both satellites carried similar broadband (0.3 - 13.0 kHz) VLF receivers with magnetic loop antennas [Rorden et al., 1966] which provided the bulk of the data for the present study. The broadband receiver output was telemetered to earth in real time on a special purpose channel and provided continuous coverage of the entire band with 80 db dynamic range. OGO 1 also recorded the broadband amplitude by means of a voltage controlled oscillator; however, its postlaunch calibration is uncertain as will be discussed in a later section. In addition to the broadband receiver designed to provide detailed spectral resolution, both satellites carried digital stepped-frequency VLF receivers to provide detailed

amplitude information over a broad (0.2 - 100 kHz) frequency range. The digital data, when processed, were used in the present study to verify hypotheses reached on the basis of the broadband data.

#### D. INTERPRETATION OF SPECTROGRAMS

VLF broadband receiver data were recorded on magnetic tape at the satellite tracking stations. For data analysis the spectrum was later displayed on film using a Rayspan spectrum analyzer. On such a spectrogram the ordinate is frequency, the abscissa is time, and the darkness of the exposure at any point varies (non-linearly) with the amplitude of the radiation.

When studying the spectrograms in this paper, the reader should keep several points in mind. Horizontal lines at discrete frequencies (e.g. 2.46 kHz) are spurious signals caused by spacecraft equipment such as the d-c to a-c converters. Temporal variations in the background level are caused by 1) an onboard amplitude compression system which adjusts the sensitivity of the receiver to the strongest signal present, and 2) for OGO 1 a 12-second periodic fading of the telemetry signal due to the spin of the spacecraft. (The spin axis was nearly parallel to that of the VLF loop antenna, and except for telemetry fading the spin had no observed effect in the data.) The time mark code at the bottom of the spectrogram is derived from the tracking station clock (WWV is usually available if greater accuracy is required). In some cases (Figures 5, 11 and 15) the amplitude VCO frequency has been translated and superimposed on the VLF spectrum. In looking at all spectrograms it is important to note the time and frequency scales, as compression or expansion of the record may change the appearance of the activity considerably.

Caution must be exercised in interpreting these records. Since the sensitivity of the OGO broadband VLF receiver increases with frequency by about 6 db per octave the higher frequencies are accentuated. Because the receiver has a log compressor action (essentially a fast AGC) only the strongest of several signals present may appear on the records. Nonlinearities inherent in photographic processing may exacerbate these difficulties. Thus strong hiss could conceal a weaker band of chorus, although chorus would not be as likely to conceal hiss (the hiss would tend to appear in any intervals between discrete chorus emissions). As another example, broadband hiss with an upper-cutoff frequency could appear banded on the records due to the decreasing sensitivity at low frequencies. In short, the apparent intensity as measured by the relative darkness of activity on the broadband spectrograms can be quite deceptive. These problems may often be overcome by referring to the digital VLF data when it is available.

## II. CHARACTERISTICS OF VLF RADIATION IN THE MAGNETOSPHERE

### A. THE DATA

The records which provided the data for the present study consist of continuous Rayspan spectrograms covering frequencies from 0.3 to 10.5 kHz, i.e., most of the range of the OGO broadband (0.3 - 13.0 kHz) VLF receiver. About 250 hours of continuous data from OGO 1 (29 passes) and OGO 3 (87 passes) were scaled according to the type of activity to determine the regions of occurrence of VLF radiation, particularly chorus, in the magnetosphere. During the 6-month period studied (June through December 1966) the satellites traversed much of the magnetosphere. The orbits are plotted in geocentric distance versus local time in Figure 1. While OGO 1 remains inside about 6 earth radii in the morning magnetosphere, it travels to sufficiently high magnetic latitudes to cover L-values up to 9 or greater at all local times.

In mapping the data the satellite was located with three parameters: dipole latitude  $\phi$ , fieldline parameter  $R_o$ , and local time LT.  $R_o$  is defined as the geocentric distance (in earth radii) to the magnetic equator crossing of the magnetic fieldline passing through the satellite. The distorted field model of Williams and Mead [1965] was used for the geometry and strength of the magnetic field. The difference between  $R_o$  and the Jensen-Cain L-value was found to be less than 10% for  $R_o < 6$ .  $R_o$  was used rather than L to emphasize the diurnal variation of the distance to the equatorial generation region of certain types of VLF noise. Geographic rather than magnetic local time was used, the difference always being less than an hour for the OGO-1 and OGO-3 orbits.



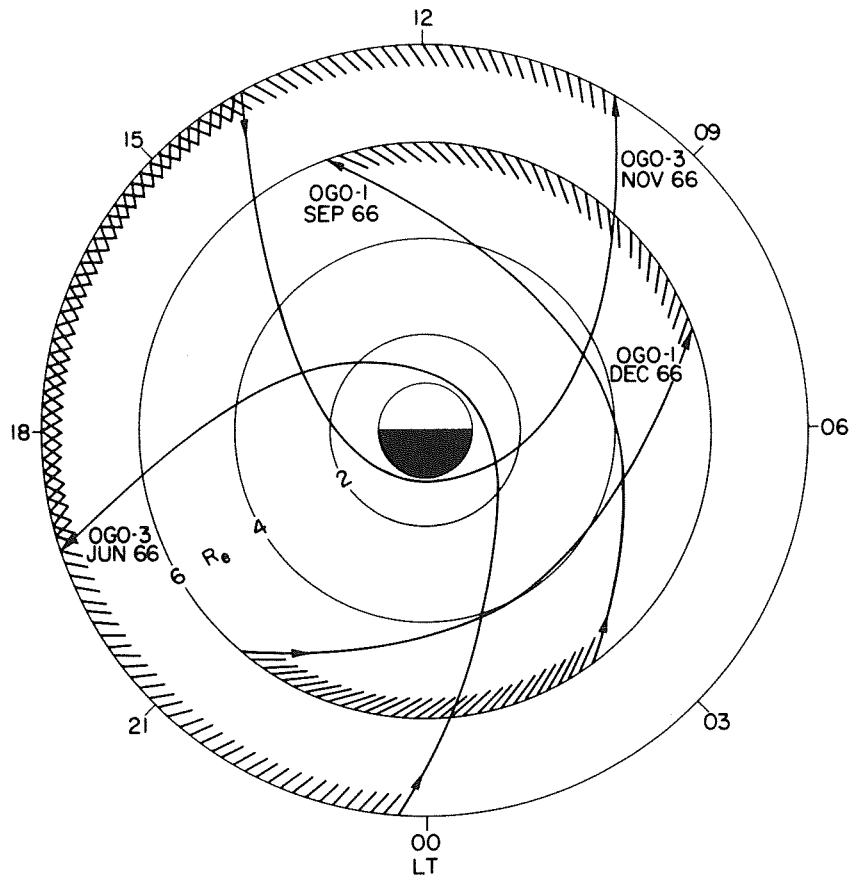


FIGURE 1. Satellite orbits for the period for which occurrence statistics were calculated:  
 OGO 1, 16 September through 8 December 1966;  
 OGO 3, 25 June through 19 November 1966.  
 Coordinates are local time LT and geocentric distance  $R_e$ .

Three types of activity were differentiated in scaling the records; these may be called banded chorus, banded hiss, and low-frequency noise. These three types include all VLF noise except whistlers commonly observed in the data under investigation. While this classification may be regarded as preliminary, it seems likely that the occurrence of each type of noise depends on significantly different physical conditions if not different processes. The differences in the three types of activity are sufficiently pronounced that an unambiguous classification can usually be made with little hesitation by the person scaling the record. These three types may be thought of as a more detailed classification of the spectral properties of emissions below the local electron gyrofrequency reported by Dunckel and Helliwell [1969] using OGO-1 digital data. Other types of activity such as "broadband noise" and "highpass noise" observed in OGO-1 digital data [Ficklin et al., 1969] were not conspicuous in the present data. Broadband noise might be difficult to distinguish from background noise in the present broadband records; highpass noise occurs above the passband of the present experiment.

Banded chorus, the first type of activity, is illustrated in Figure 2. It consists of discrete, sometimes overlapping narrowband emissions whose center frequency  $f$  lies between approximately 0.1 and 0.6 times the minimum (equatorial) gyrofrequency  $f_{Ho}$  on the fieldline passing through the satellite. The emissions tend to occur in a single band within this range; the apparent bandwidth may vary widely but is most often between 10% and 50% of the center frequency. As the satellite moves in to lower  $R_o$ , this band of emissions moves to higher frequencies corresponding to the increased gyrofrequency (magnetic field)

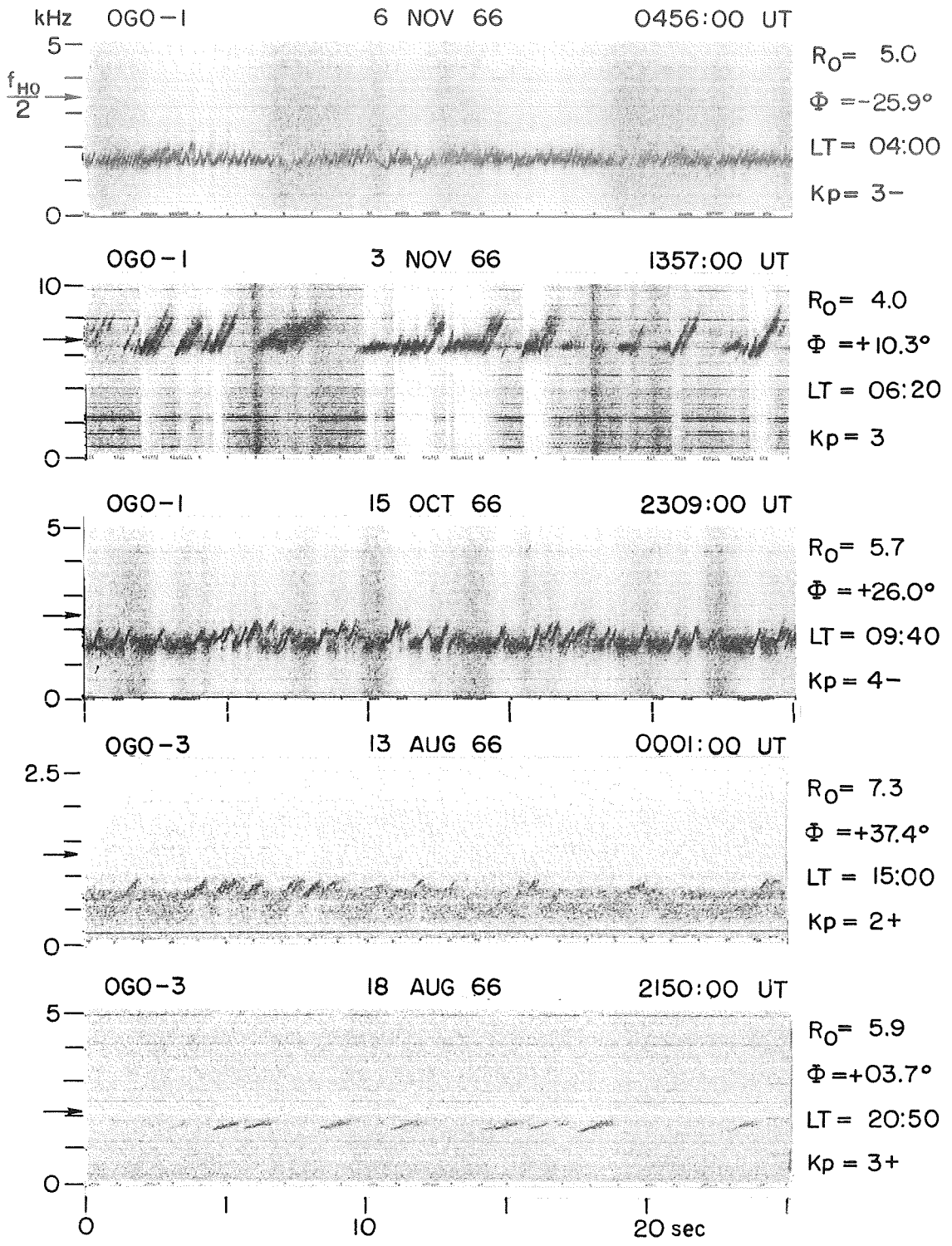


FIGURE 2. Examples of banded chorus, showing the confinement of discrete emissions to a single frequency band. Vertical and horizontal striations are interference as discussed in the text. The arrow on the frequency scale marks  $f_{Ho}/2$  (Williams-Mead model). Satellite coordinates and 3-hour  $K_p$  are given on the right. The banded chorus is accompanied by  $p$  hiss in the third and fourth example.

at the equator [Burtis and Helliwell, 1969]. The individual discrete emissions in this band may be of any spectral shape (risers, falling tones, "hooks", etc.) but typically one shape is dominant for any given time period on the order of an hour. The "chorus" made up of these discrete emissions appears similar to that recorded for many years at ground stations, but occurs in a limited frequency range whereas ground-observed chorus often occurs in several bands over a wide range of frequency (e.g., Helliwell [1965], figures 7-35, 7-43, 7-58, etc.). Banded chorus was found to be the most common type of VLF activity in the high  $R_o$  region, generally beyond the plasmopause.

Banded hiss, the second type of activity, is illustrated in Figure 3. It consists of an unstructured band of noise occurring in the same frequency range ( $0.1 < f/f_{Ho} < 0.6$ ) as banded chorus. By definition there are no narrowband, discrete emissions discernable in pure banded hiss; however, it is often accompanied by banded chorus as in the last two examples of Figure 3. Banded hiss is not as common as banded chorus but occurs in a roughly similar region.

Low-frequency noise, the last type of activity, is shown in Figure 4. It consists of noise well below the banded chorus frequency, and with further study could perhaps be differentiated into several categories. Most often it is simply broadband hiss extending from the lowest frequencies on the record (about 300 Hz) to an upper cutoff of perhaps  $0.1 f_{Ho}$ . However, the upper cutoff does not always follow the minimum gyrofrequency as the satellite moves in  $R_o$ ; often during a given pass the frequency remains constant over a wide range of  $f_{Ho}$ . Sometimes the noise does not extend down to 300 Hz, but in all cases

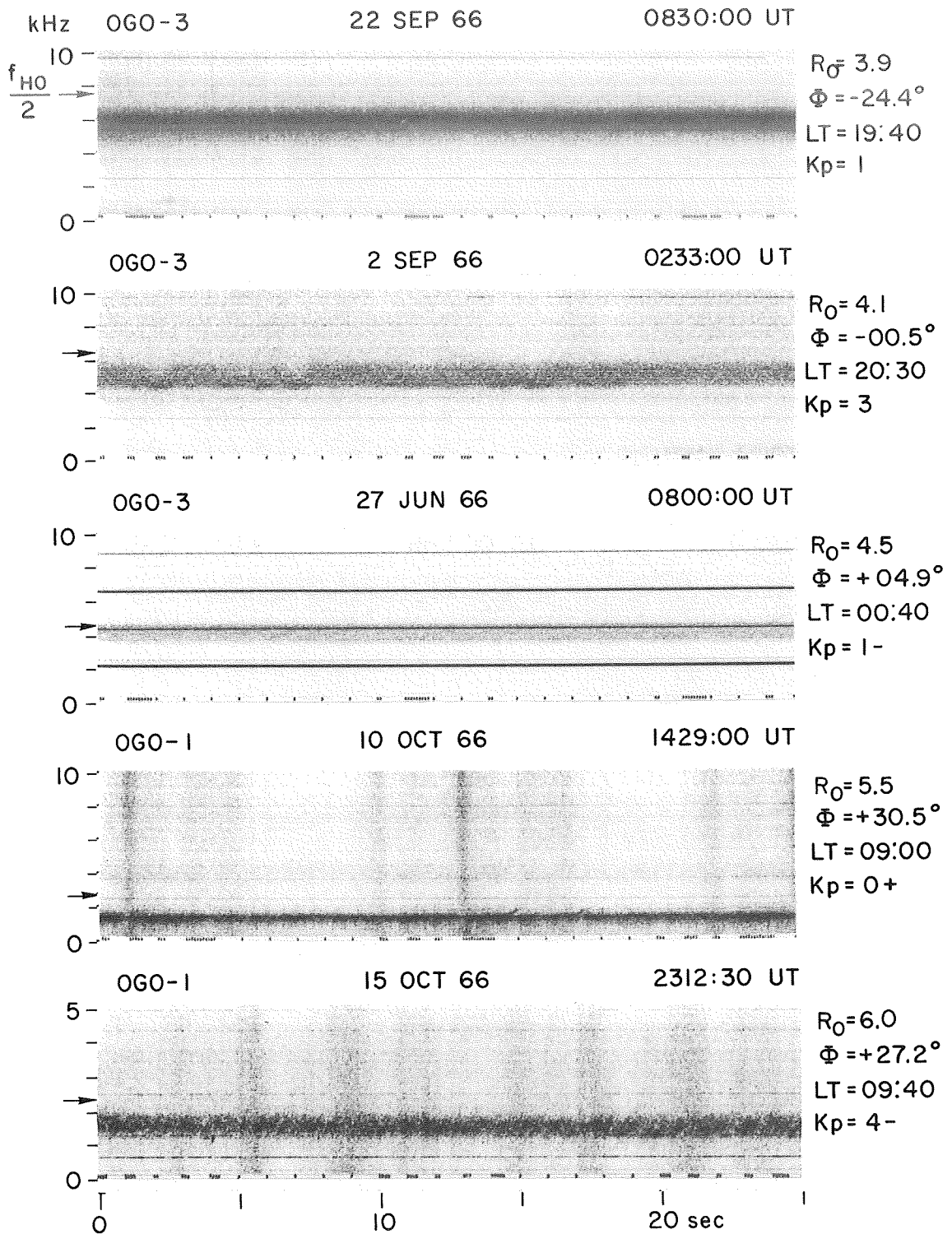


FIGURE 3. Examples of banded hiss, showing the confinement of non-structured activity to a single frequency band somewhere between 0.1 and 0.6  $f_{HO}$ . Some structured banded chorus is also present in the last two examples. In the 27 June record the horizontal lines are at multiples of one-quarter the measured local gyrofrequency

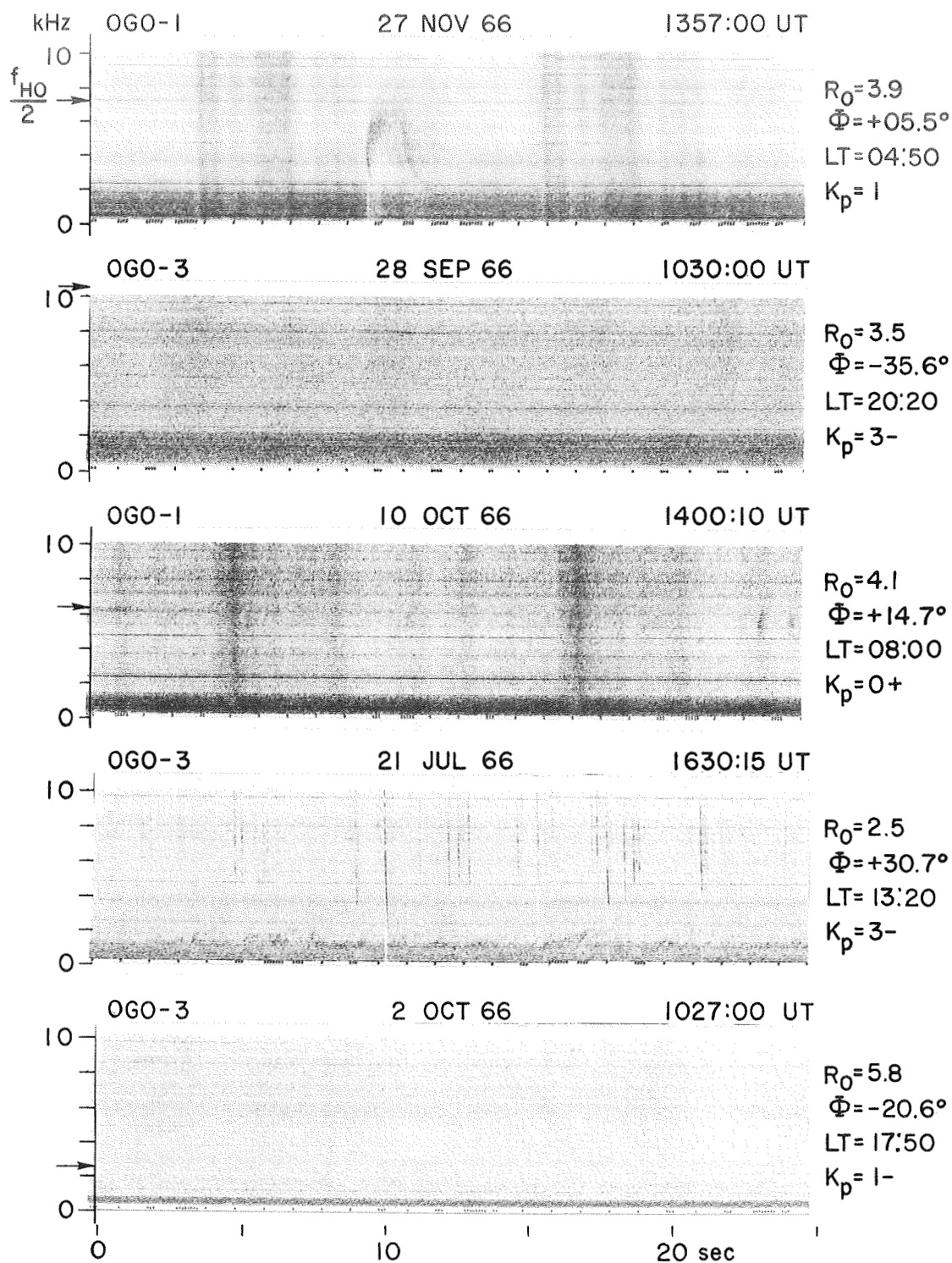


FIGURE 4. Examples of low-frequency noise. Note that activity is far below the  $f_{HO}/2$  arrow (off scale in the fourth example) and extends to the low frequency cutoff of 300 Hz. Whistlers are also present in the first, third and fourth examples.

the lower cutoff is far below  $0.1 f_{Ho}$ . Only rarely are there discrete emissions within the low-frequency hiss. Low-frequency noise was found to be the most common type of VLF activity (excepting whistlers) in the low  $R_o$  region, generally within the plasmasphere.

These three types of noise were defined and scaled according to their appearance on the broadband spectrograms. As mentioned in the previous chapter these spectrograms must be interpreted with caution. For instance, broadband noise with an upper-cutoff frequency could appear banded in the records due to the decreasing sensitivity of the OGO broadband VLF receiver at lower frequencies. The examples in Figures 2 and 3 were chosen from the 1966 data for which occurrence statistics were calculated. Unfortunately digital data are not yet processed for this period, and we cannot be certain that the activity in these examples is truly banded. However the lower cutoff of banded chorus and banded hiss is usually quite abrupt, and appears to be sharper than the 6 db per octave rolloff of the receivers (the hiss in the fourth example of Figure 2 may be an exception). In any case, earlier 1965 digital data confirm the existence of truly banded noise. During the inbound OGO-1 passes of March through May 1965, both banded chorus and banded hiss are commonly observed in the broadband and digital data.

A representative example of this simultaneous digital and broadband data is given in Figure 5. Typical banded chorus may be seen in the lower half of the broadband spectrogram, with activity extending from about 2.5 to greater than 4.0 kHz. The broadband amplitude, to be discussed below (Section F), is indicated by the upper trace on the spectrogram. A single frame from the band 1 and band 2 digital stepping receivers is

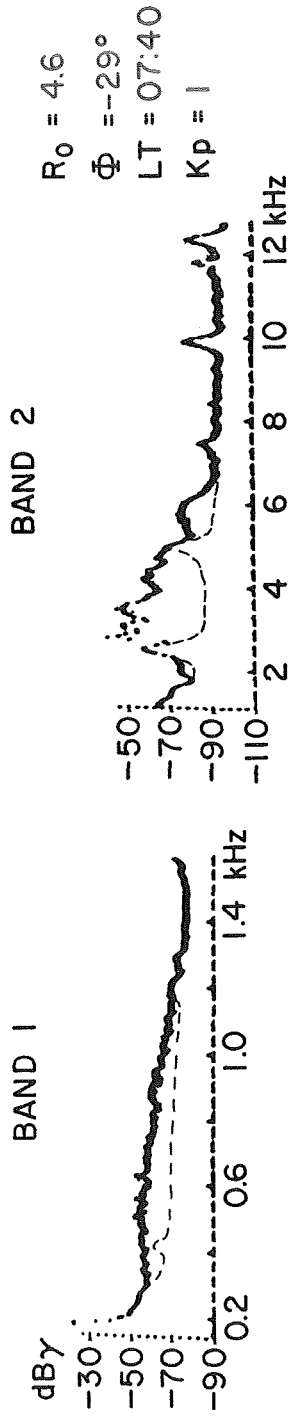
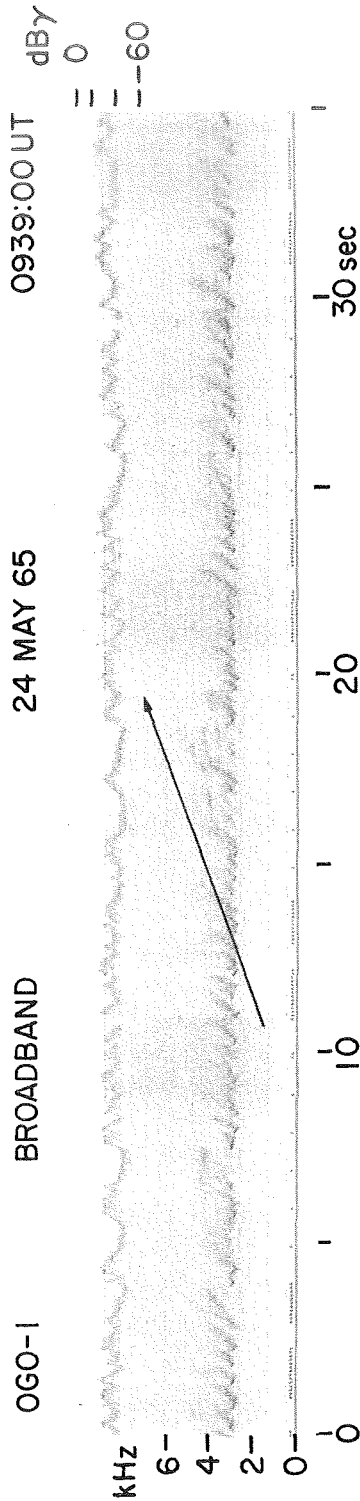


Figure 5. Simultaneous data from the broadband receiver and the band 1 and band 2 digital sweeping receivers on OGO 1. The broadband amplitude trace inserted above the banded chorus activity at  $\sim 3$  kHz is tentatively calibrated in db below one gamma. The arrow traces the first part of the band 2 frequency sweep shown below. Dashed lines on the digital records indicate the noise level; amplitude is in db below one gamma over the filter bandwidth ( $\sim 40$  Hz, band 1;  $\sim 160$  Hz, band 2). Banded radiation is evident on the band 2 receiver. Noise below 1.2 kHz on the band 1 receiver is not observed on the broadband spectrogram due to receiver characteristics discussed in the text.



shown below; the first part of the band 2 frequency sweep for this frame is traced by the arrow on the spectrogram. The noise level of the digital receivers is indicated by the dashed lines. Activity may be seen on the band 2 receiver between about 2 and 7 kHz, strongest at about 2.8 kHz; this corresponds to banded chorus. The separate peaks of the amplitude trace are caused by the receiver stepping through successive emissions. As for most cases of banded chorus and banded hiss which have been compared with digital data, there is a definite low-frequency cutoff, and the activity is certainly banded.

A separate band of activity may be seen on the band 1 receiver between about 0.3 and 1.2 kHz. While this is only slightly weaker than the banded chorus it does not appear at all on the broadband spectrogram. This illustrates how the decreased sensitivity of the broadband receiver at low frequencies, coupled with the receiver AGC and non-linear photographic processing, may cause low-frequency activity to be obscured on the broadband spectrograms. This activity on the band 1 receiver seems to be independent of the banded chorus and on other occasions does not appear although banded chorus or banded hiss is evident in the digital data. It seems similar to low-frequency noise as defined above. Dunckel and Helliwell [1969], using digital data from the first 100 passes of OGO 1 (September 1964 - May 1965), found that in the magnetosphere as a whole the strongest VLF radiation occurred below 500 Hz 84% of the time.

To map the occurrence of each type of activity, the 1966 broadband data were sorted into eight 3-hour blocks in local time (LT) and seven 1-unit increments in  $R_o$ . The number of passes in each compartment of  $R_o$  - LT space varied from 7 to 32 (the few compartments having fewer than 7 passes were considered to have insufficient data for statistical

purposes and are indicated by dashed lines in Figure 7). If, during a pass, a type of activity occurred anywhere in the compartment it was considered an "occurrence" (typically if activity was present it lasted over several compartments). The number of passes having an "occurrence" divided by the total number of passes then determined the percentage occurrence for each compartment.

Figure 6 shows the satellite orbits and activity for one representative 3-hour period, 2100 - 2400, plotted in the meridional plane. The fieldlines are those of the Williams-Mead model for this local time period. Solid lines indicate those portions of passes having no VLF activity; x's indicate banded chorus activity; cross hatches indicate banded hiss activity; and circles indicate low-frequency noise activity. Compared to other local times the occurrence of VLF activity during this period is relatively low.

The percentage occurrence for the three types of activity is presented in Figure 7 as a function of  $R_0$ , for the eight different local time blocks. By scanning from the top of the figure downward, the radial movement of the region of maximum occurrence throughout the day may be visualized. The similarity of the regions of occurrence of banded chorus and banded hiss is evident, as is the dissimilarity of the region of occurrence of low-frequency noise. The following sections will discuss the occurrence statistics for each type of activity in turn.

#### B. BANDED CHORUS

A single band of discrete emissions between about 0.1 and 0.6 times the minimum gyrofrequency on the fieldline passing through the

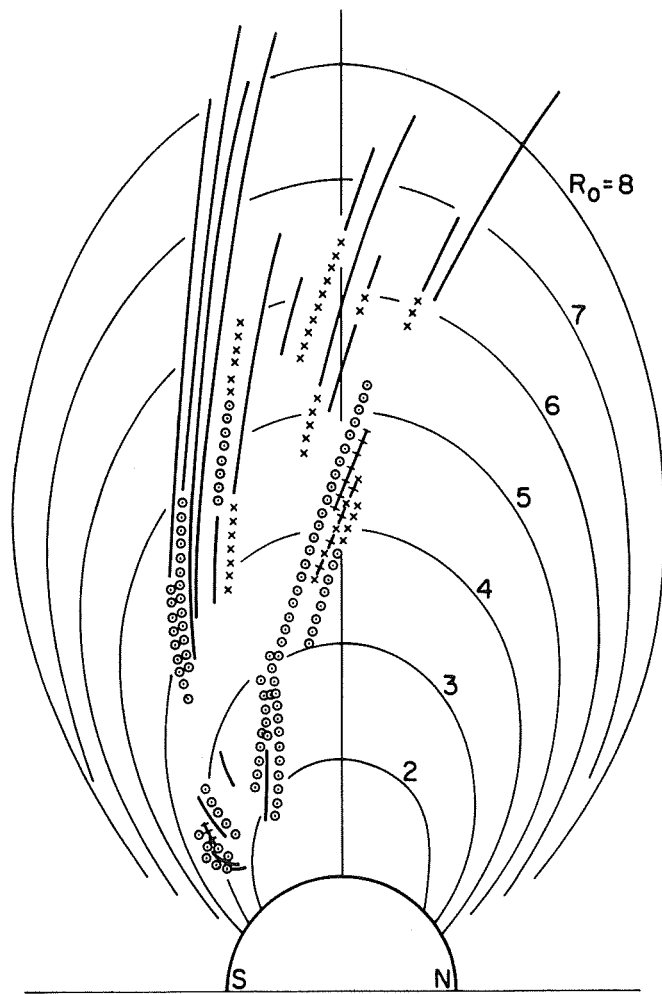


FIGURE 6. Satellite orbits and activity for one representative 3-hour local time block (2100-2400 LT). X's represent banded chorus, hatch-marks banded hiss, circles low-frequency noise, and solid lines no activity.  $R_0$  is the magnetic equator crossing distance of the magnetic field-line (Williams-Mead model).

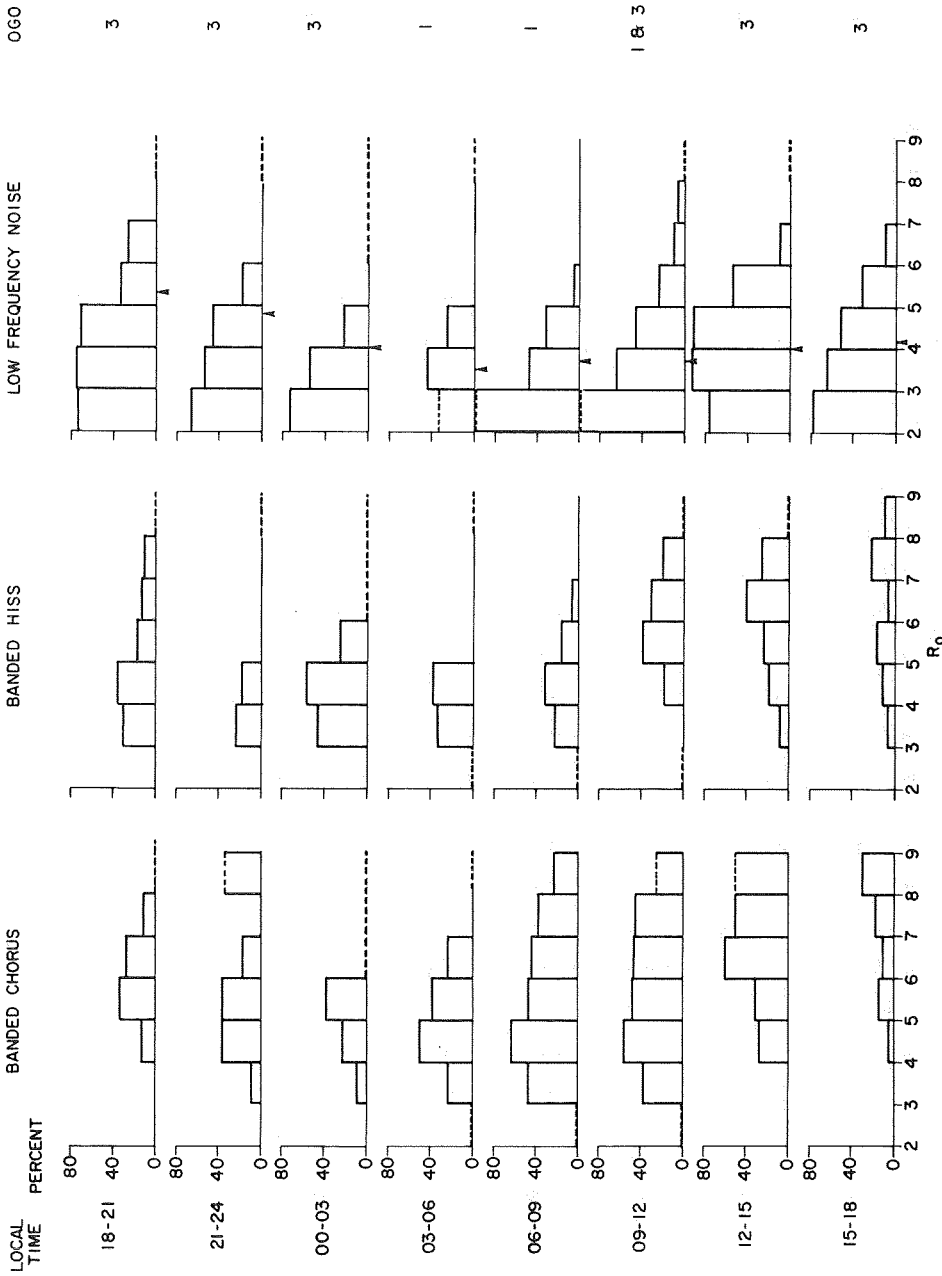


FIGURE 7. Occurrence statistics for three types of VLF radiation, as a function of  $R_0$  and local time. Dashed lines indicate occurrence based on limited data. Arrows on the  $R_0$  scale for low-frequency noise mark Carpenter's [1966] average position of the plasmopause. The satellite providing the bulk of the data for each time period is shown on the right.

satellite is the most common type of activity at  $R_o$  greater than 4 or 5. As shown in Figure 7, the occurrence of banded chorus depends on local time and  $R_o$ . Although banded chorus is observed at all local times, it is most common in the morning, from 0300 to 1500 LT, when it is present about 50% of the time. The region of maximum occurrence moves out from  $R_o = 4 - 5$  before 0600 to  $R_o > 6$  after 1200. During the late afternoon chorus is at a minimum, but activity increases again after 1800 and the zone of maximum occurrence moves slowly inward until the common morning activity begins. Although the statistics showing chorus to be most common during the morning are based simply on the presence or absence of activity, the morning activity also tends to be stronger and more continuous than the evening activity, as suggested by the examples in Figure 2.

Further perspective is gained by plotting the occurrence statistics for banded chorus in the equatorial plane (Figure 8). The plane is divided into the same compartments as the data, i.e., 3-hour blocks of local time and 1-unit increments of  $R_o$ . Regions having insufficient data (fewer than seven passes) are unshaded; light shading indicates 0 - 20% occurrence; diagonal hatching indicates 20 - 40% occurrence; and heavy shading indicates 40 - 62% occurrence. The curve of  $x$ 's marks an average position of the plasmopause for moderately disturbed conditions as determined from 1963 whistler observations [Carpenter, 1966]. Also shown (for two locations) is the parallel energy of resonant electrons under the assumption of transverse cyclotron resonance and a model ambient number density in the equatorial plane.

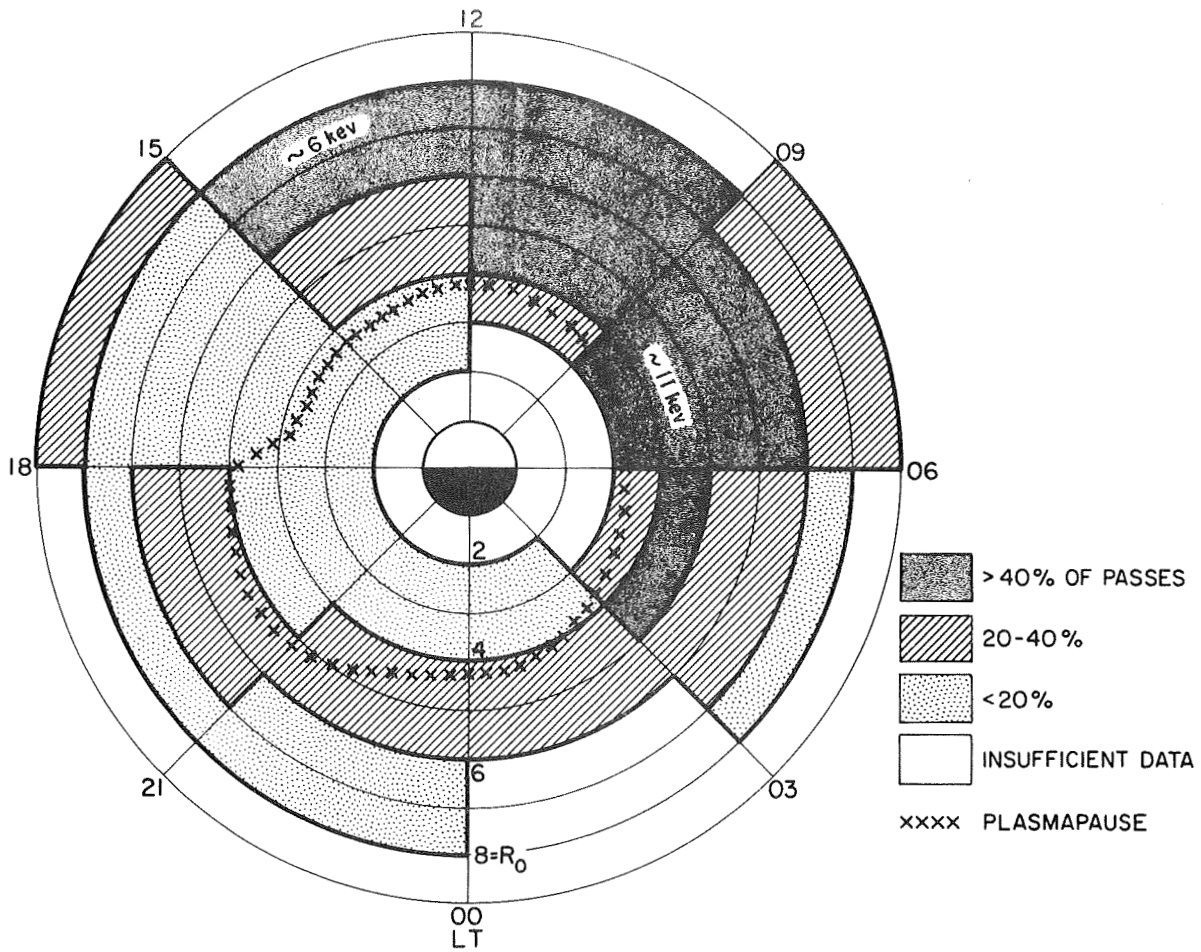


FIGURE 8. Occurrence of banded chorus as a function of  $R_0$  and local time plotted in the equatorial plane. Light shading indicates 0-20% occurrence, diagonal hatching 20-40%, and heavy shading 40-62%. Insufficient data in unshaded regions. The curve of X's marks Carpenter's [1966] average plasmopause position. Parallel energies of gyroresonant electrons are calculated as in the text.

It has been shown [Burtis and Helliwell, 1969] that there is reason to believe that banded chorus is generated near the equator and propagates approximately parallel to magnetic fieldlines. Figure 8 may then be interpreted as showing that the principal generation region lies beyond the plasmopause, and moves out farther from the earth later in the morning, perhaps reaching as far as the magnetopause during early afternoon. The corresponding change in L-value is slightly greater than the change in  $R_0$  since the field is more compressed in the noon meridian. This locus of maximum occurrence is reminiscent of calculated drift paths of  $\sim 1 - 10$  keV electrons assuming an east-to-west electric field across the magnetosphere [Brice, 1967; Kavanagh et al., 1968]. This region is also similar to the region where Carpenter [1966, Figure 12] found the largest number of whistlers beyond the plasmopause, although this number is still **small** compared to the number of whistlers within the plasmasphere. Whistlers were not seen in this region in the present study, suggesting the satellites did not pass through active ducts during the period studied. This supports the conclusion of Burtis and Helliwell [1969] that banded chorus is generally non-ducted.

It is often assumed that the generation mechanism for discrete VLF emissions basically involves gyroresonance between the circularly polarized whistler-mode waves and electrons gyrating along magnetic fieldlines [Brice, 1964b; Helliwell, 1967]. Applying the resonance condition that electrons see a wave frequency Doppler-shifted to their gyrofrequency by their parallel velocity, and using the empirical observation that the banded chorus frequency is close to half the

equatorial gyrofrequency [Burtis and Helliwell, 1969], we obtain

$$f = \frac{v_p}{v_p - v_{\parallel}} \quad f_H = \frac{1}{2}f_H$$

where  $f$  = wave frequency

$f_H$  = electron gyrofrequency

$v_p$  = wave phase velocity

$v_{\parallel}$  = electron velocity parallel to magnetic field.

This implies  $v_{\parallel} = -v_p$ , i.e., the parallel velocity of resonant electrons is equal to the phase velocity of the waves but in the opposite direction.

The parallel energy of resonant electrons can be found by substituting the well-known expression for whistler-mode phase velocity and recalling that  $f = f_H/2$ :

$$E_{\parallel} = \frac{1}{2}m_e v_p^2 = \frac{\frac{1}{2}m_e c^2}{1 + \frac{f_o^2}{f(f_H - f)}} = \frac{255.5 \text{ keV}}{1 + 4\left(\frac{f_o}{f_H}\right)^2}$$

where  $E_{\parallel}$  = parallel kinetic energy of resonant electrons

$m_e$  = electron mass

$c$  = speed of light

$f_o$  = plasma frequency.

Using the Williams-Mead model to determine  $f_H$  and the whistler measurements of Angerami and Carpenter [1966] to determine  $f_o$ , values of  $E_{\parallel}$  are found to be on the order of 10 keV throughout most of the region where banded chorus is most common. Vasyliunas [1968] has reported large fluxes of electrons with spectral energy peak somewhat above 1 keV outside the plasmopause prior to 0600 LT, with gradually



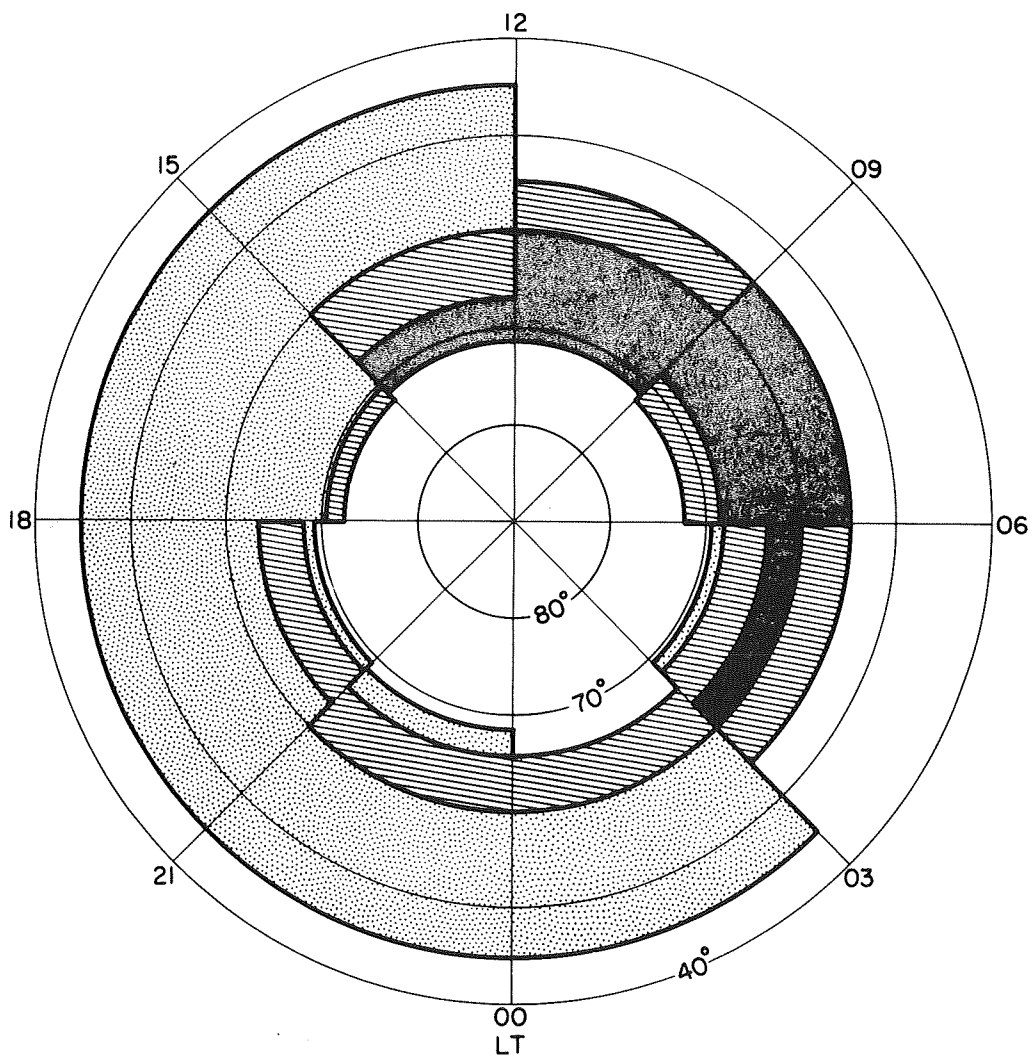


FIGURE 9. Occurrence of banded chorus as a function of quasi-invariant latitude QINV and local time. QINV was determined by tracing the Williams-Mead fieldline from its equator crossing  $R_0$  to its intersection with the earth. Note that low  $R_0$  data blocks cover a wider range of QINV. Shading as in Figure 8.

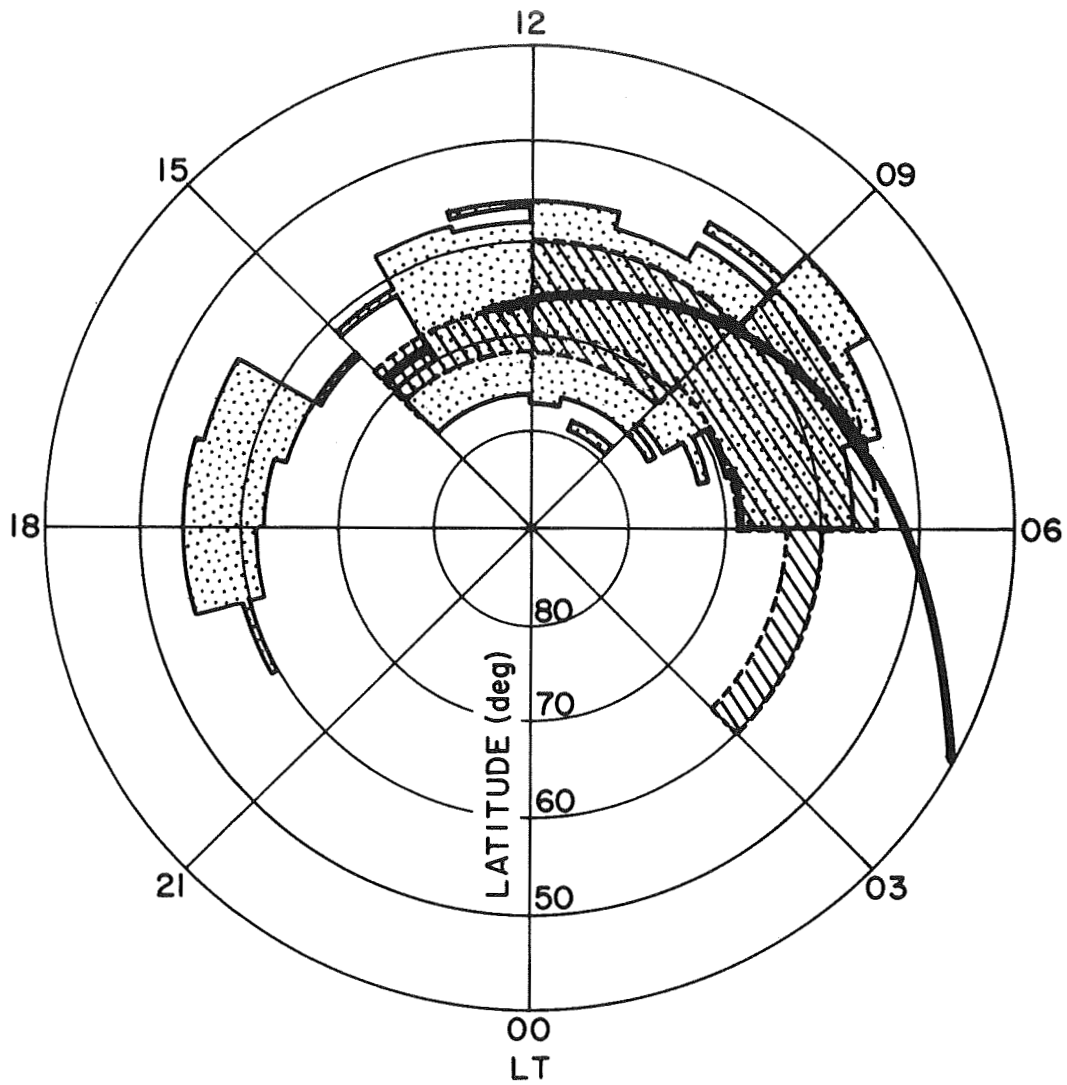


FIGURE 10. Comparison of occurrence of VLF chorus. The diagonally hatched region is based on OGO-1 and OGO-3 occurrence of banded chorus as a function of QINV. The dotted region is based on Injun-3 topside ionosphere VLF data [Taylor and Gurnett, 1968] as a function of true invariant latitude. The heavy curved line is based on ground observations of chorus [Pope, 1963] as a function of "eccentric latitude." See text.

decreasing fluxes later in the morning. Banded chorus and associated precipitation may be an important loss mechanism for these particles.

To facilitate comparison with high-latitude ground measurements, the occurrence statistics for banded chorus are converted from  $R_o$  to an equivalent quasi-invariant latitude (QINV) and presented in Figure 9. QINV was found by tracing the Williams-Mead fieldline through the satellite to its intersection with the earth (QINV as defined here does not include internal field harmonics and so is not strictly true invariant latitude). Note that low  $R_o$  data blocks cover a comparatively wide range of QINV, and because of variations in field compression the high  $R_o$  blocks cover different QINV at different local times. Regions having occurrence from 0 - 20%, 20 - 40%, and 40 - 62% are shaded as in Figure 8. This presentation should be especially useful for correlation with particle precipitation, x-ray microburst, and low altitude VLF experiments.

The banded chorus occurrence statistics are compared with topside ionosphere and ground station VLF chorus statistics in Figure 10. The diagonally hatched region is where OGO 1 and OGO 3 most commonly observed banded chorus (40 - 62% of the passes). The dotted region is where Taylor and Gurnett [1968] report 0.2 - 7.0 kHz magnetic field strengths exceeding 1.8 milligammas more than 20% of the time on Injun 3 in the topside ionosphere, regardless of the type of activity, plotted as a function of true invariant latitude. The heavy curved line is where Pope [1963] reported the local time of maximum chorus activity (aurally scaled) for ground stations at various eccentric latitudes (eccentric latitude is obtained by centering the geographic latitude grid on the geomagnetic pole).

The Injun-3 data in Figure 10 include all types of VLF noise and thus are not directly comparable with data on discrete emissions alone. However, the data after 1600, at lower invariant latitudes, are thought to be primarily what Taylor and Gurnett call "ELF hiss", by analogy with OGO observations here of low-frequency noise.\* The remainder of the Injun-3 data are thought to be a mixture of ELF hiss and VLF chorus. The region of occurrence is nevertheless roughly comparable with that of magnetospheric banded chorus.

Figure 10 shows a moderately good correlation between the OGO data and Pope's ground data. Both show a similar tendency for the peak chorus occurrence to move to higher latitudes later in the morning. The ground maximum appears to be at slightly lower latitudes than the magnetospheric maximum. This may be related to increased ionospheric absorption of VLF frequencies at high latitudes. The apparent discrepancy before 0600 is partly explained by the fact that chorus occurred much less frequently for this portion of Pope's curve. Laaspere et al. [1964] found the local time of maximum chorus occurrence to be constant at about 0600 for ground stations below  $55^{\circ}$ , becoming later only at higher latitude stations. They also reported an abrupt decrease in chorus occurrence below  $50^{\circ}$  magnetic latitude.

Russell et al., [1969] using the search-coil magnetometer on OGO 3, have recently reported two distinct classes of activity at frequencies between 10 and 800 Hz: "steady noise" and "noise bursts". When the lower frequency range of their experiment as compared to the present is considered, the occurrence region of "noise bursts" appears to be roughly consistent with that of banded chorus.

---

\* This question is currently being investigated.

The similarities between discrete emissions observed in the magnetosphere (banded chorus) and discrete emissions observed for many years at ground stations include (1) the same overall frequency range, (2) roughly similar spectral characteristics, and (3) similar regions of occurrence with respect to magnetic shell and local time. Ground observed chorus differs from banded chorus in that (1) it often occurs in several bands over a wide range of frequency, and (2) it often appears to be triggered by whistlers. If it is assumed that banded chorus is generally non-ducted [Burtis and Helliwell, 1969], then it should not be possible for the radiation to reach low altitudes [Thorne and Kennel, 1967]. Indeed, it has proved to be very difficult to match identical emissions on the satellite and ground records. As will be reported in a separate paper, what is believed to be nonducted banded chorus is occasionally observed on the low altitude satellite OGO 2. Most of the chorus seen in the topside ionosphere and on the ground, however, is tentatively interpreted as banded chorus radiation which was generated in or later became trapped in the same type of ducts that allow whistlers to penetrate the ionosphere.

### C. BANDED HISS

A band of unstructured noise at the same frequency as banded chorus is often observed both with and without the latter. As shown in Figure 7, the region of occurrence of banded hiss is generally similar to that of banded chorus, with activity confined to relatively low  $R_0$  at night and moving outward during the daytime hours. Hiss was observed less frequently than chorus in the morning, 03 - 15 LT, but during the rest of the day the two were about equally likely. It was found that the

peak occurrence of banded hiss was at slightly lower  $R_0$  than the peak occurrence of banded chorus for most local times. The general similarity of banded chorus and hiss in terms of frequency and region of occurrence suggests combining them into a single category of VLF radiation. The percentage occurrence for this combined category is less than the sum of percentage occurrence for banded chorus and banded hiss, however, since the two often occurred simultaneously and hence are not mutually exclusive.

The combination of banded hiss and banded chorus at low frequencies, as in the fourth example of Figure 2 and the last two examples of Figure 3, is similar in appearance to the 0.5 - 1.5 kHz "polar chorus" observed at high latitude ground stations and described by Ungstrup and Juckerott [1963]. While these authors suggested that polar chorus might be fundamentally different from the higher frequency chorus observed at lower latitude ground stations, the present study shows a continuous range of frequency of chorus as a function of magnetic shell in the magnetosphere. Other distinguishing features of polar chorus noted by Ungstrup and Juckerott include later local time of occurrence (consistent with OGO observations at these frequencies), negative correlation with  $K_p$  (perhaps due to ionospheric absorption), and more pronounced seasonal variation (as might be expected at high latitudes). It seems likely that both polar chorus and lower latitude ground-observed chorus are manifestations of magnetospheric banded chorus and hiss.

#### D. LOW-FREQUENCY NOISE

Noise below about 0.1 times the minimum electron gyrofrequency on the fieldline through the satellite, usually extending down to the

300 Hz low-frequency cutoff of the equipment, was found to occur in a distinctly different region than banded chorus and banded hiss. Figure 7 shows that low-frequency noise was observed on about 70% of the passes regardless of local time inside  $R_0 = 4$ . The arrows in Figure 7 indicate Carpenter's [1966] average position of the plasmopause, and it is clear that low-frequency noise is common in the higher density plasma region inside this boundary. It is less clear that the apparent drop in occurrence outside the plasmopause is real. Because the broadband receiver discriminates against low frequencies, higher frequency banded chorus and hiss may often obscure low-frequency noise beyond the plasmopause as suggested by Figure 5. As previously mentioned, Dunckel and Helliwell [1969] found the strongest radiation usually to occur below 500 Hz, typically within the range of low-frequency noise, even beyond the plasmopause. On the other hand, banded chorus is often intermittent or entirely absent on the broadband records from this region, yet low-frequency noise does not appear even when the AGC has increased the receiver gain. While it is probably true that low-frequency noise is less common outside the plasmopause than inside, the decrease in occurrence is probably not as abrupt as indicated in Figure 7.

Low-frequency noise seldom shows any discrete structure; it is usually hiss. Of 214 samples with low-frequency noise activity, only 22 were found to have discrete, narrowband emissions in the same frequency range. These cases occurred at a median  $R_0$  of 3.7, and the average frequency of the emissions was  $0.09 f_{Ho}$ . In one case the emissions seem to have been reflected at low altitudes since they were seen first at a ground station and later on the satellite.

Taylor and Gurnett [1968], using the low altitude satellite Injun 3, report a type of noise they call "ELF hiss" which seems to be similar to low-frequency noise. It is slowly-varying "hiss with frequency components from a few hundred Hz up to about 2 kHz" and is the most common strong VLF radiation observed on Injun 3. Russell et al. [1969] also report "steady noise" at frequencies below 1 kHz on OGO 3 which seems to be similar to low-frequency noise. They observe steady noise primarily at L-values less than 6 but also above  $L = 6$  at high magnetic latitudes on the dayside. The generation and propagation of low-frequency noise is an interesting problem but due to measurement difficulties inherent in the broadband receiver it was not pursued further in the present study.

#### E. COMPARISON OF OGO-1 AND OGO-3 DATA

It is important to check whether the particular satellite used to gather the data has any effect on observed activity since OGO 1 and OGO 3 supplied data for separate regions of the magnetosphere. In particular, data from 12 LT through the evening to 03 LT were predominantly OGO 3, while data from 03 to 09 LT were predominantly OGO 1, as indicated in Figure 7. The period 09 to 12 LT had about 15 passes from each satellite over a wide range of  $R_o$ , and was used to check for independence. The test showed generally good agreement between the satellites in trends and even in values of percentage occurrence, considering the limited number of passes. The following differences were noted for the 09 to 12 LT period:

1. Banded chorus peaked at slightly lower  $R_o$  on OGO 1. This is the same trend shown in Figure 7; however, the outward shift between 06 - 09 (OGO 1) and 12 - 15 (OGO 3) is much



greater than the difference between OGO 1 and OGO 3 found here from 09 - 12. Therefore the outward shift is believed to be real.

2. Banded hiss was somewhat more common for all  $R_o$  on OGO 3. If hiss is always more common on OGO 3, the period 03 - 09 LT (OGO 1) might be expected to show a decrease in hiss. Since it does not seem to, the increased occurrence on OGO 3 from 09 - 12 is attributed to statistical fluctuation.
3. Low-frequency noise fell off faster with  $R_o$  on OGO 3. This is the opposite to the trend shown in Figure 7, where for 03 - 09 (OGO 1) the low-frequency noise falls off faster than for most other time periods.

It is therefore concluded that the data are substantially free of bias from the two different satellites, which are supposed to have essentially the same instrumentation. Differences in the data, as noted above, are minor; the major diurnal trends shown in Figure 7 are thought to be real.

#### F. AMPLITUDE OF BANDED CHORUS

The OGO 1 VLF experiment includes a voltage controlled oscillator (VCO) whose frequency deviation was designed to be approximately proportional to the logarithm of the broadband (0.3 - 13.0 kHz) amplitude [Rorden et al., 1966].\* Unfortunately the absolute values of the VCO frequency in flight are not the same as the prelaunch values; this may be related to an unexpected thermal environment caused by the spacecraft's spin or to a component failure. By autumn 1966 the VCO sync frequency had settled down to a constant 35.1 kHz, as compared to 32.2 kHz before launch: a 9% increase. According to one of the designers [B. Ficklin, private communication] it is not unreasonable to assume that the in-flight deviation from sync to the measured value

---

\* The VCO was employed on OGO 3 to provide ELF (15 - 300 Hz) waveforms.

is then also 9% greater than the prelaunch deviation for the same amplitude. The prelaunch calibration curves, suitably modified by the above assumption, then yield a preliminary estimate of broadband amplitude. This estimate is conservative in the sense that the amplitude obtained by the modified calibration curves is less than that obtained using the prelaunch curves; the difference approaches 10 db at the largest signal strengths. Nevertheless, the preliminary estimates of amplitude obtained by this method seem quite large and may have to be revised downward. While there is uncertainty in the absolute values of amplitude thus obtained, dynamic amplitude variations such as rise and fall time should be quite accurate. The VCO response time is approximately 3 msec, determined by a post-detection 300 Hz low-pass filter in the VCO channel.

The amplitude VCO has been inserted above the banded chorus activity in Figure 5 and tentatively calibrated by the above assumption. The broadband amplitude is seen to range between about 20 and 40 db below one gamma ( $1\gamma = 10^{-5}$  gauss). The digital data in Figure 5 show the narrowband amplitude in db below one gamma over the digital receiver filter bandwidth (band 1,  $\sim 40$  Hz; band 2,  $\sim 160$  Hz) for each step in the frequency sweep. When this narrowband amplitude data is integrated over the frequency range of the broadband receiver, a broadband amplitude of -34 db  $\gamma$  is obtained for this particular sweep. This is consistent with the tentative calibration of the broadband VCO. Most of the power (67%) is contained in the banded chorus between 2.7 and 3.7 kHz; low-frequency noise from 0.3 to 1.0 kHz accounts for another 27%. Whereas the most important contribution to the average wideband intensity

for the entire magnetosphere has been found to lie below 500 Hz [Dunckel and Helliwell, 1969], this example shows that the strongest contribution can at times lie elsewhere; in particular, at banded chorus frequencies.

Figure 11 shows some representative banded chorus emissions and their amplitude variations. The amplitude VCO is tentatively calibrated, under the above assumptions, in db below one gamma. The apparent noise level and calibration depend on the frequency of the radiation because of the 6 db/octave frequency response of the broadband receiver. The first and second spectrograms were calibrated for  $f = 1.8$  kHz, the third for  $f = 6.7$  kHz. Since the frequency of the emissions is actually varying, for example, by over one octave in the second spectrogram, the indicated calibration should be increased by about 3 db for  $f = 1.3$  kHz, and decreased by about 6 db for  $f = 3.6$  kHz. The regular, rapid oscillations of the VCO at about 1357:17 on 3 November 1966 result from the internal calibration signal consisting of a square wave at harmonics of 1 kHz.

The peak amplitudes of the emissions, as determined by the tentative calibration, range from the noise level to about 100 milligammas, and occasionally higher. These examples were chosen from among the stronger emissions found, and more commonly the amplitude would probably not exceed 100 milligammas. Nonetheless, these (tentative) amplitude peaks often exceed the levels calculated by Kennel and Petschek [1966] as being necessary for steady pitch angle diffusion by radiation well below the electron gyrofrequency. Figure 11 shows that the emissions typically build up to a peak value of short duration and then decay.

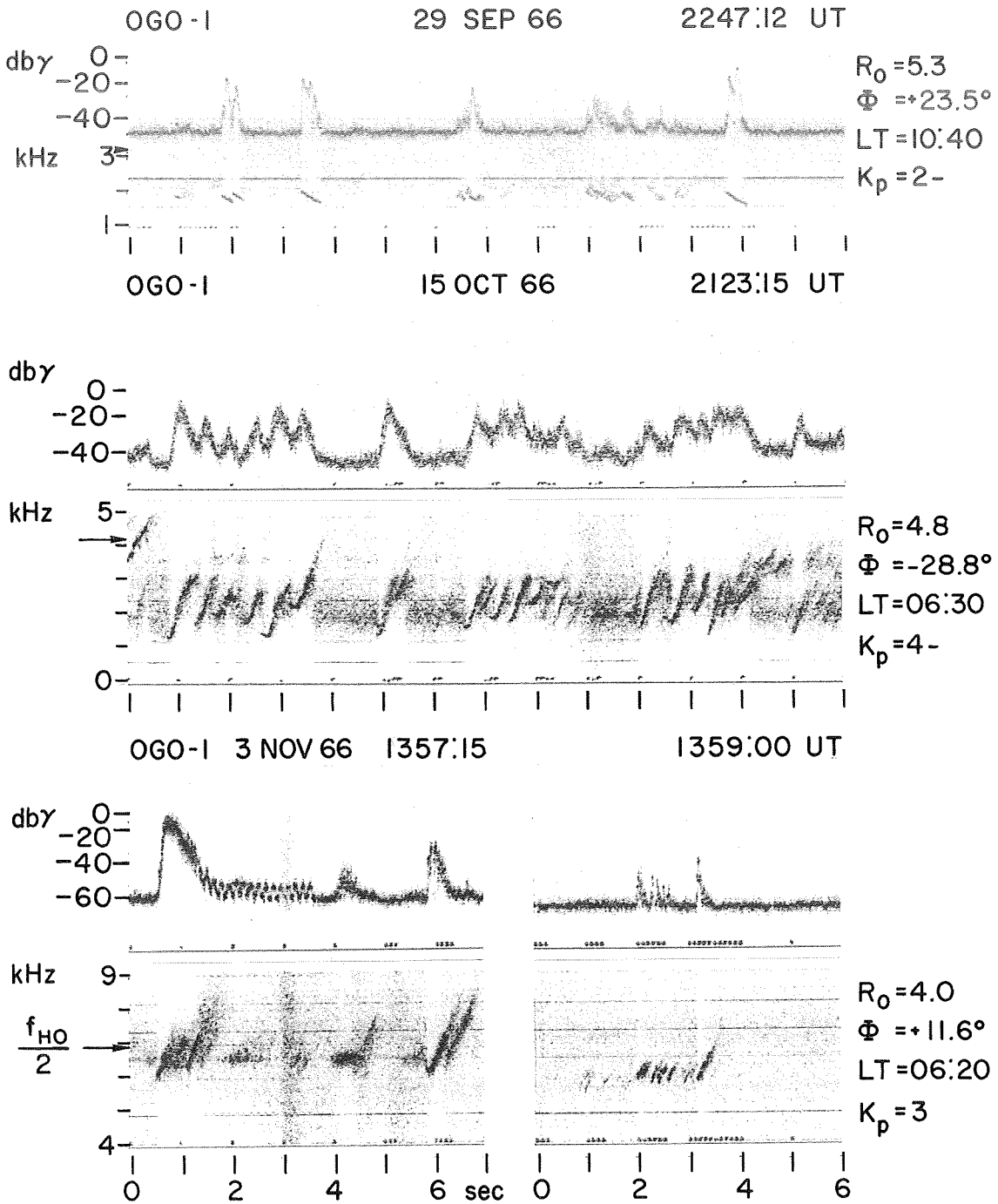


FIGURE 11. Examples of the amplitude variation of banded chorus emissions observed by OGO 1. The broadband amplitude, tentatively calibrated in db below one gamma, is shown above the corresponding VLF spectrogram. The regular oscillations in amplitude on 3 November are due to an internal calibration signal at 1 kHz and harmonics. Banded hiss is present with the chorus on 15 October.

The rise time is usually, but not always, shorter than the decay time. The last emission of the 29 September example shows an unusual double peak in amplitude. The short duration of maximum amplitude is in contrast to Lee's [1968] spectral analysis of emissions observed at ground stations, which show a relatively long duration of near-maximum amplitude. These banded chorus amplitude spikes appear similar to the X-ray microburst spikes reported by Venkatesan et al. [1968], which may result from electrons precipitated by the banded chorus emissions.

#### G. LATITUDE DEPENDENCE

The dependence of VLF activity on magnetic dipole latitude  $\Phi$  was in general found to be less pronounced than the dependence on  $R_0$  and LT. Figure 12 gives the percentage occurrence for the three types of radiation as a function of  $\Phi$  for various values of  $R_0$ . In order to obtain a significant number of samples it was necessary to use data from a wide range of local times: banded chorus data were taken from 03 - 15 LT (the time of maximum occurrence), banded hiss data from the same 03 - 15 LT period, and low-frequency noise data from 09 - 21 LT (again approximately the time of maximum occurrence). Dipole latitude  $\Phi$  was divided into  $10^\circ$  intervals;  $R_0$  into 1-unit increments. Percentage occurrence was found by dividing the number of passes having activity by the total number of passes in each compartment of  $\Phi - R_0$  space. The number of passes in each compartment for which percentage occurrence was calculated varied from 8 to 47. The remaining compartments (having 0 - 5 passes) were considered to have insufficient data for statistical purposes and are indicated by x's in Figure 12.

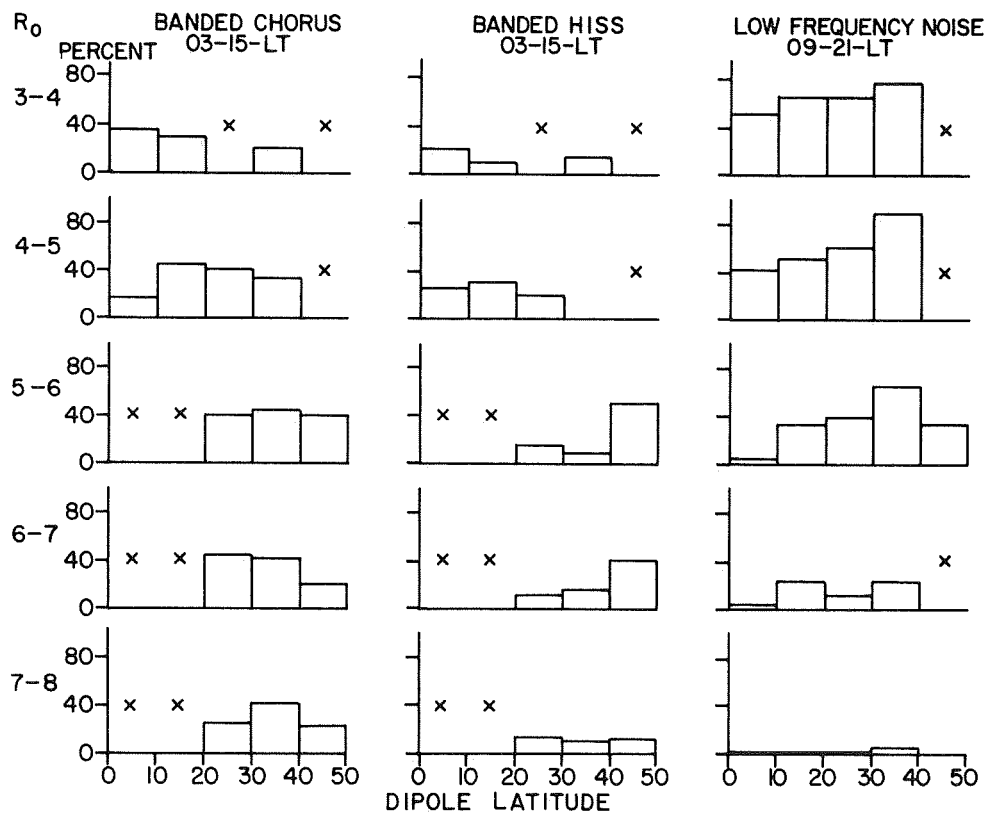


FIGURE 12. Occurrence statistics for three types of VLF radiation as a function of dipole latitude  $\phi$  for various  $R_0$ . The local time period is shown at the top. An X indicates insufficient data (5 or fewer passes) in given  $\phi - R_0$  compartment.

Banded chorus occurrence showed no consistent dependence on latitude. All variations in percentage occurrence with latitude (Figure 12) are thought to be attributable to the limited data sample. Russell et al., [1969], using the OGO-3 search-coil magnetometer, report a decrease in occurrence of "noise bursts" (from 10 to 800 Hz) with latitude. Their data show this to be significant, however, only at L-values greater than 7 in which region processed broadband data for the present experiment are relatively sparse. In this region the latitude dependence may be partially due to the increased path length from the equator to a given latitude, or to the fact that by ordering their data in L rather than  $R_o$  they are not including the effects of solar wind distortion of the geomagnetic field.

Banded hiss occurrence likewise showed no consistent dependence on latitude. The anomalously high percentage occurrence found for  $\Phi = 40 - 50^\circ$  between  $R_o = 5$  and 7 is based on only 10 passes and may not be statistically significant.

Low-frequency noise, however, was found to be consistently more common at high latitudes, as shown in Figure 12. This trend is clearly evident for  $R_o$  less than 6 ; beyond  $R_o = 6$  the observation of low-frequency noise is uncommon at any latitude (Figure 7). Russell et al. [1969] noted a similar high-latitude preference for "steady noise" below 800 Hz on OGO 3.

While the occurrence of banded chorus was found to be essentially independent of latitude, the normalized frequency of banded chorus,  $f/f_{Ho}$ , was found to depend on latitude as suggested by Figure 13. This data is from a separate study [Burtis and Helliwell, 1969], including OGO-1 and OGO-3 passes from 1965 - 1967 over a wide variety of

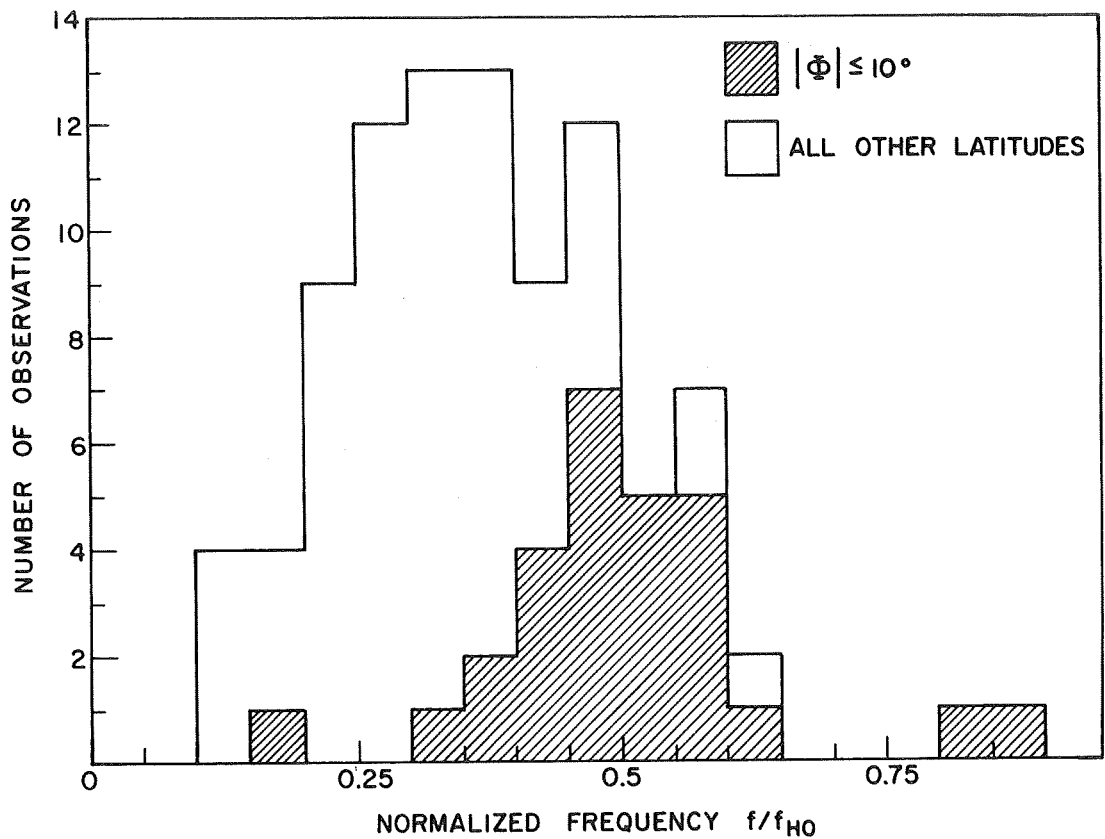


FIGURE 13. The number of observations of banded chorus at various normalized frequencies for dipole latitudes  $\Phi$  within  $10^\circ$  of the equator and for all other dipole latitudes. The banded chorus center frequency  $f$  is normalized to the equatorial gyrofrequency on the Williams-Mead fieldline through the satellite,  $f_{H0}$ . The data sample is that of Burtis and Helliwell [1969] and includes a wide variety of passes from 1965 - 1967.



orbits. When all latitudes were considered the banded chorus center frequency  $f$  was typically anywhere in the range  $0.1$  to  $0.6 f_{Ho}$ , but when dipole latitudes were within  $10^\circ$  of the equator  $f$  was typically between  $0.4$  to  $0.6 f_{Ho}$ . The normalized frequency was found not to depend on  $R_o$ . This was interpreted as a propagation effect in which nonducted banded chorus deviates slightly inward from magnetic fieldlines while traveling earthward from a generation region near the equator.

#### H. DEPENDENCE ON MAGNETIC ACTIVITY

All 28 OGO-1 passes in the 0600 - 0900 local time period were studied to investigate the dependence of the three types of VLF activity on magnetic disturbance. Worldwide 3-hour values of  $K_p$  measuring magnetic agitation, and 1-hour values of  $D_{st}^*$  measuring symmetric, longitude-independent depression of the field were used as magnetic parameters. The data were divided into consecutive 5-minute time segments and the type of VLF activity, location of the satellite in  $R_o$ , and magnetic activity were noted for each segment, giving 397 data-samples (33 hours of data). In order to qualify as a statistically meaningful data point in  $R_o - K_p$  (or  $R_o - D_{st}$ ) space at least 12 data-samples including at least 4 separate passes were required. Points not meeting this criterion are indicated by dashed lines in Figure 14.

During the autumn 1966 period for which the data were obtained there were at least four well-defined magnetic storms exhibiting a short interval of increased  $D_{st}$ , a sudden drop of 50 to 100 gamma, and a slow, quasi-exponential recovery to  $D_{st} \cong 10$ . Values of  $D_{st}$  ranged from -38 to

---

\*  $D_{st}$  values provided by World Data Center A, Rockville, Maryland.

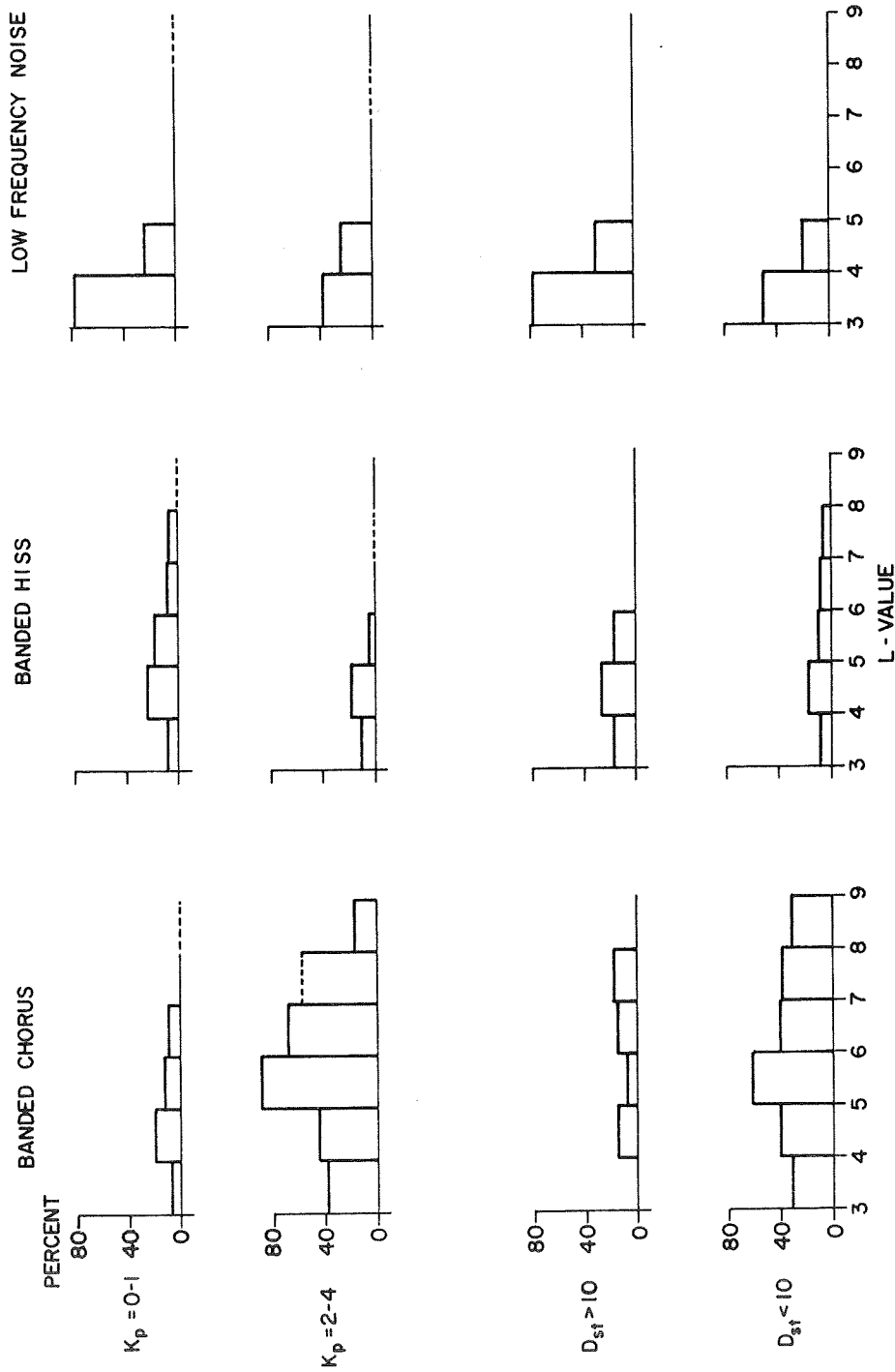


FIGURE 14. Occurrence of three types of VLF radiation between 0600 and 0900 local time as a function of  $R_o$  for magnetically quiet and moderately disturbed periods. Three-hour  $K_p$  values obtained from Lincoln [1967];  $D_{st}$  values (measuring longitudinally symmetric depression of geomagnetic field) were supplied by World Data Center A.

+37 with 32% of the samples having  $D_{st} \geq 10$  (little or no field depression) and 68% having  $D_{st} < 10$  (significant field depression). Values of  $K_p$  ranged from 0 to 6 with 51% of the samples having  $0 \leq K_p \leq 1^+$  (magnetically quiet), 44% having  $2^- \leq K_p \leq 4^+$  (moderately disturbed), and 5% having  $5^- \leq K_p \leq 6$  (magnetically active).

It was found that the occurrence of banded chorus depended markedly on magnetic activity, whether measured by  $K_p$  or  $D_{st}$ . Figure 14 shows that banded chorus occurred much more commonly for moderately disturbed periods ( $K_p = 2 - 4$ ) than for quiet periods ( $K_p = 0 - 1$ ) for all  $R_o$ . For  $R_o = 5 - 6$  the frequency of occurrence jumped from 13% (quiet) to 89% (moderately disturbed), and over the entire region  $R_o = 3 - 9$  the banded chorus activity increased from 12% to 49%. There seemed to be a slight tendency for chorus to spread to higher  $R_o$  with increased  $K_p$  as suggested in Figure 14. The two passes during magnetically disturbed periods ( $K_p = 5 - 6$ ) covered only high  $R_o$  regions but exhibited chorus activity over 50% of the time for  $R_o = 6 - 9$ . Banded chorus showed a similar dependence on  $D_{st}$ , the frequency of occurrence over the entire region increasing from 9% for  $D_{st} \geq 10$  to 39% for  $D_{st} < 10$ . In a study of VLF chorus observed at ground stations, Pope [1963] reported a similar positive correlation between  $K_p$  and occurrence, except at auroral latitudes where ionospheric absorption may be expected.

Banded hiss and low-frequency noise were found to be less dependent on magnetic activity (Figure 14). The occurrence of banded hiss actually decreased from about 14% for  $K_p = 0 - 1$  to 9% for  $K_p = 2 - 4$ . (Banded hiss behaved similarly with regard to  $D_{st}$ ,

being slightly more common for  $D_{st} \geq 10$  than for  $D_{st} < 10$  .) Low-frequency noise also was observed more often during magnetically quiet periods, especially for low  $R_o$  . For  $R_o = 3 - 4$  low-frequency noise was observed 76% of the time with  $K_p = 0 - 1$  , but only 38% of the time with  $K_p = 2 - 4$  .

Banded chorus activity for the 06 - 09 LT period is further described in Table 1 and Figures 15 and 16. The table gives a concise description of the spectral shape, purity and strength of individual discrete emissions making up banded chorus for each pass of OGO 1. Figure 15 shows spectrograms of the banded chorus activity for 5 of these passes, arranged in order of decreasing  $K_p$  . Note that the amplitude VCO trace inserted above the VLF activity is uncalibrated and its relative sensitivity is doubled in the second spectrogram. Figure 16 presents the values of  $D_{st}$  for a 3-week period bracketing many of the above passes; in particular passes a, b, c, and d refer to the top four spectrograms of Figure 15.

From the above illustrations it is seen that weak and scattered emissions, often diffuse and fuzzy, tended to occur during magnetically quiet times, whereas strong and continuous, often sharply defined emissions tended to occur during moderately disturbed times. Furthermore, at least for the period studied, falling tones and quasi-constant tones were more common for  $K_p = 0 - 1$  , whereas risers and hooks were more common for  $K_p = 2 - 4$  . Passes during the main phase of magnetic storms shown in Figure 16 had strong banded chorus activity, while those during the initial and recovery phases showed less marked activity, as might be expected from the correlation between  $K_p$  and  $D_{st}$  .

TABLE 1. BANDED CHORUS ACTIVITY, OGO 1, 06-09 LT.

	DATE 1966	$R_o = 3-6$	$R_o = 6-9$
$K_p = 0-1$	9/21	Occasional triggered periodics and quasi-constant tones	None
	10/02	Falling tones	*
	10/10	Short falling tones	*
	10/13	Fuzzy risers	*
	10/18	Bursts of risers	None
	10/21	None	*
	10/23	Quasi-constant tones	*
	11/08	Short falling tones trigger risers	None
	11/11	Fuzzy risers	None
	11/14	None	None
	11/16	Dots	None
	11/22	None	None
	11/24	None	None
11/27	*	Risers	
$K_p = 2-4$	9/16	None	*
	9/24	None	*
	9/27	Many risers	*
	9/29	Risers and falling tones	Risers
	10/07	Bursts of falling tones	None
	10/15	Many strong risers and hooks (large $\Delta f$ )	None
	10/26	Many risers and hooks	Many strong risers and hooks
	10/31	Many strong risers	Many strong risers
	11/03	Risers and falling tones	*
	11/06	Risers	Risers
	11/16	*	None
	11/19	Risers	Risers
11/27	*	Risers	
$K_p = 5-6$	11/30	*	Many risers
	12/02	None	Occasional risers

\* No data

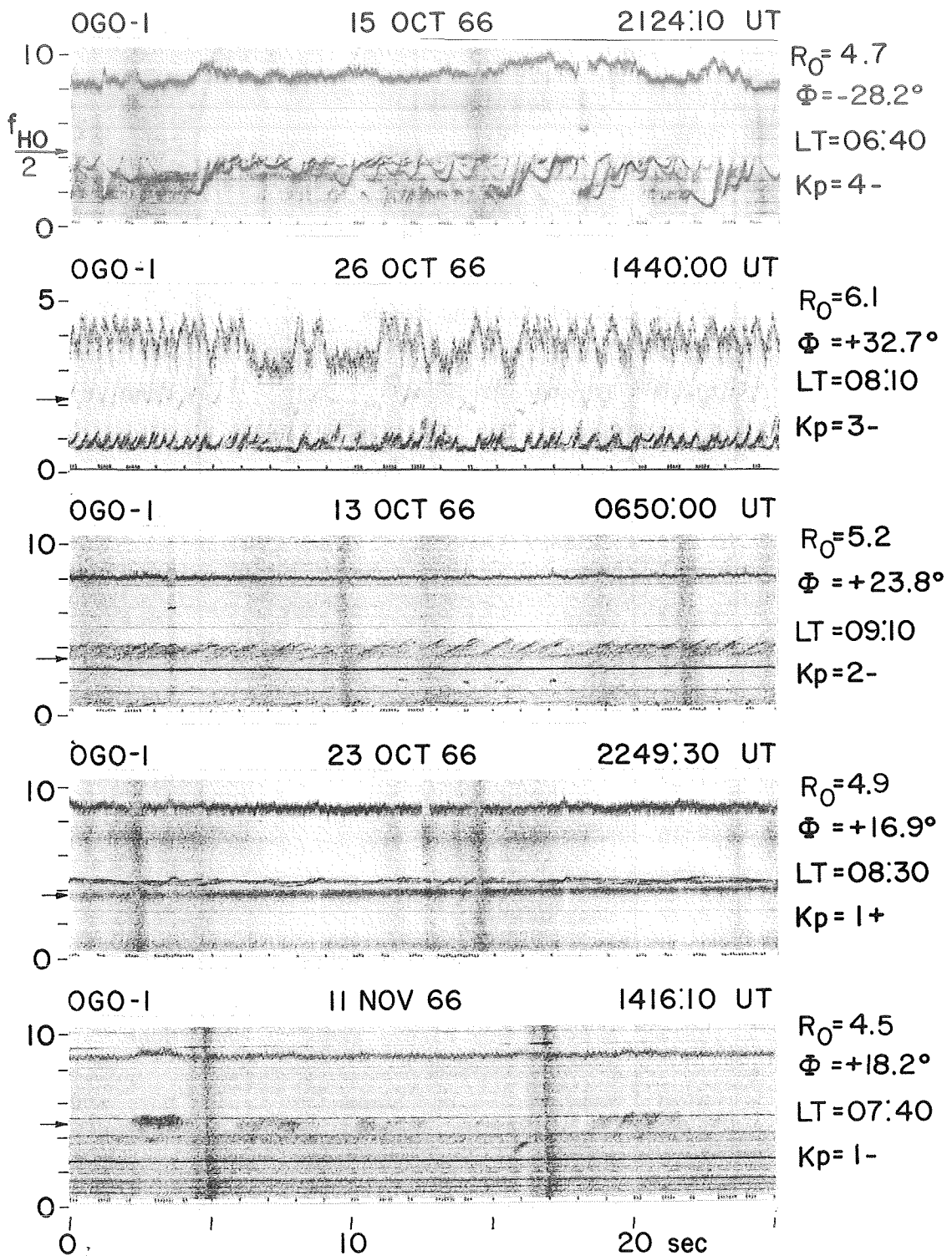


FIGURE 15. Examples of banded chorus for varying degrees of magnetic disturbance (higher  $K_p$  at the top). The broadband amplitude trace is uncalibrated<sup>p</sup> but appears between 8 and 10 kHz (in the second example it appears between 2.5 and 4.5 kHz and the sensitivity is doubled; in the third example the noise level is lower because an interfering experiment was off). These examples are among those summarized in Table 1.

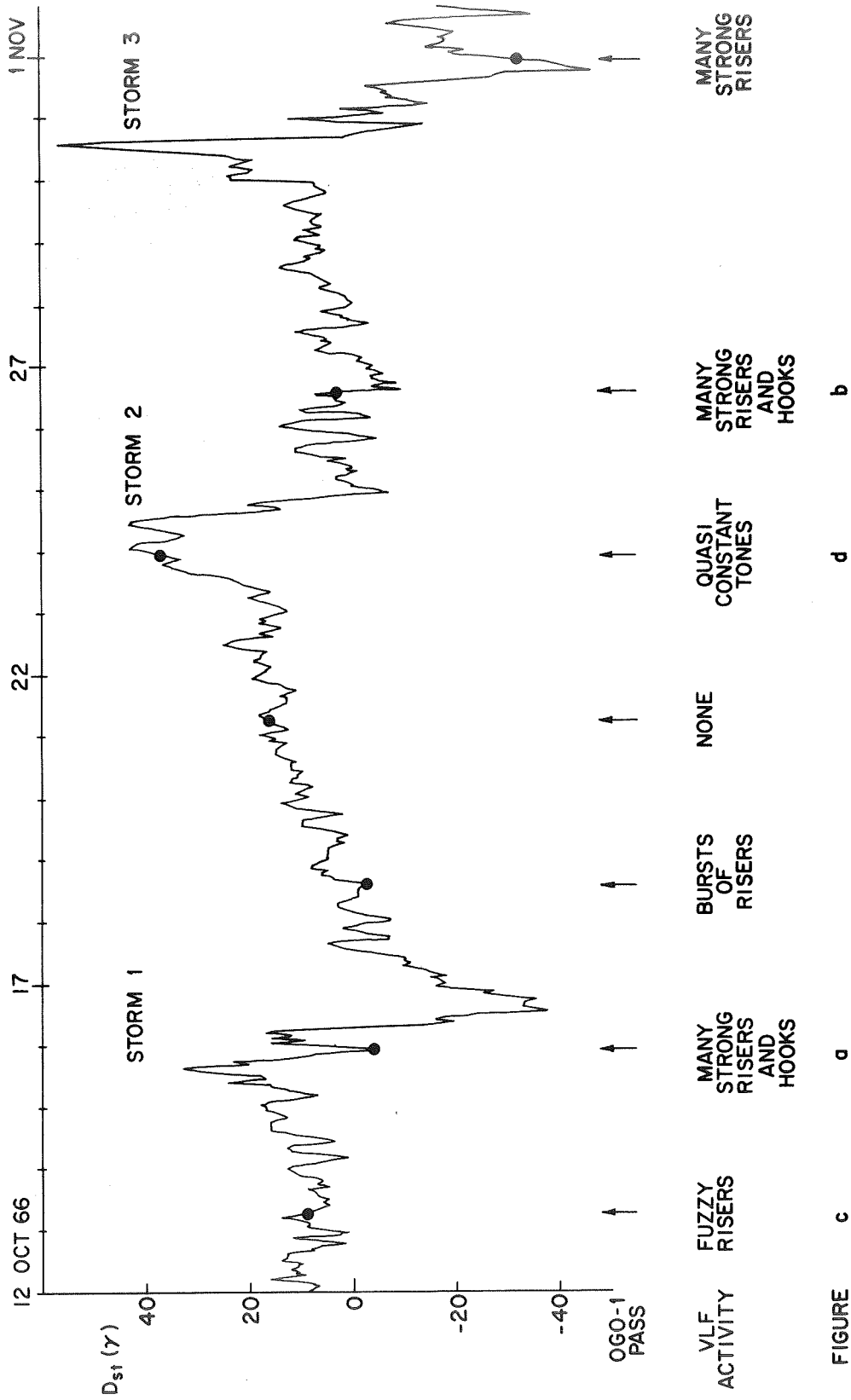


FIGURE 16.  $D_{st}$  values for a 3-week period in October 1966, with a concise description of the VLF banded chorus activity observed by OGO 1 during its relatively brief passages through the (morning) magnetosphere. Portions of passes a, b, c, and d are illustrated in the first four examples of Figure 15 (a at the top).

## I. AN UNUSUAL OBSERVATION OF NOISE ABOVE THE GYROFREQUENCY

On a single occasion narrowband VLF radiation was observed in the magnetosphere at frequencies well above the expected local electron gyrofrequency. This unique event occurred on 10 September 1966 as OGO 3 was crossing the dipole equator and moving inward from  $R_o = 5.9$  to  $R_o = 5.2$  at about 2000 local time. Figure 17 shows the orbit and the various regions of activity. Before 0357 UT no activity is seen. For the next 22 minutes strong bands of noise are observed both above and below the local gyrofrequency. Then from 0419 to 0445 UT the only noise band is well below the local gyrofrequency, and in fact is just below half the equatorial gyrofrequency as would be expected for banded chorus. The banded chorus increases in frequency as the satellite moves inward until at 0445 it ceases and soon thereafter whistlers begin to appear.

The radiation above the electron gyrofrequency (as given by the Williams - Mead field) appears in several narrow bands of slowly and irregularly varying frequency and amplitude. The various bands fade in and out and apparently are not harmonically related. They are usually diffuse but occasionally discrete structure can be seen. Figure 18 shows a spectrogram of these noise bands as well as two frames of data (from a slightly different time) from the VLF digital stepping receiver on the same satellite. The horizontal bands of nearly constant frequency are the activity of interest on the spectrogram -- at least two such bands may be seen above the local gyrofrequency  $f_H$ . The digital data present magnetic field strength (db below one gamma) vs. frequency (kHz) for three frequency bands. In the second frame, for example, there is



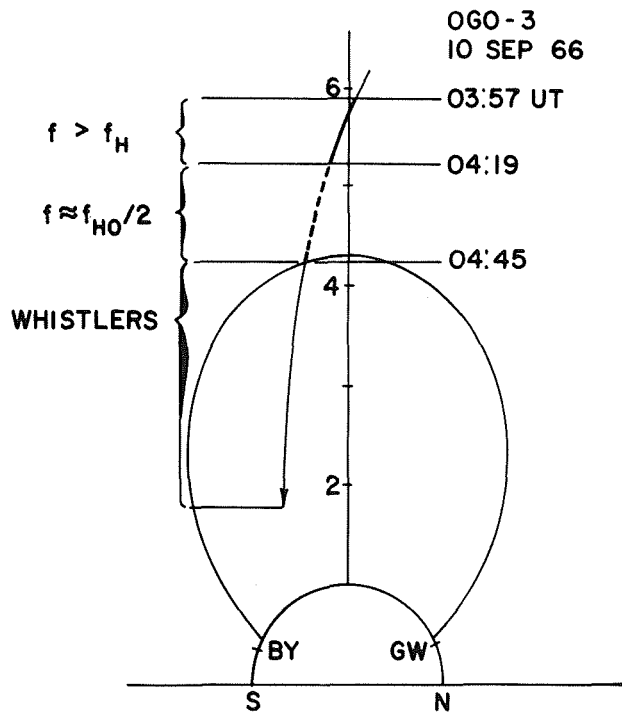
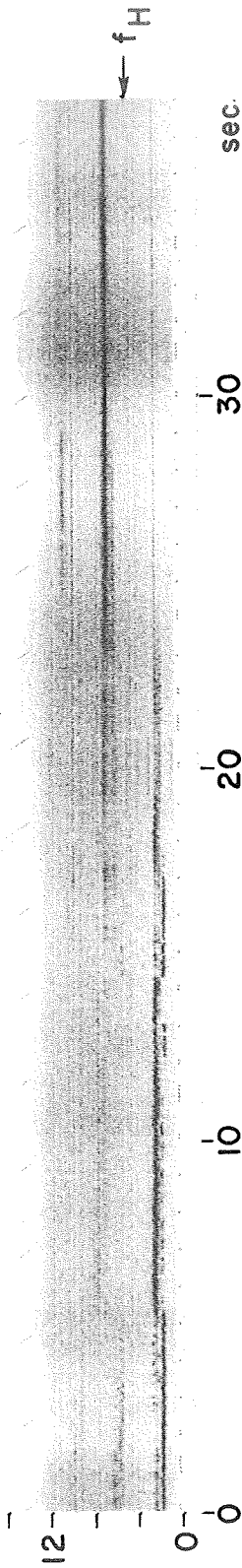


FIGURE 17. OGO-3 orbit for 10 September 1966, during part of which radiation was observed above the local (Williams-Mead) gyrofrequency  $f_H$ . The field-line shows the approximate location of the plasmopause. VLF activity is indicated at the left.

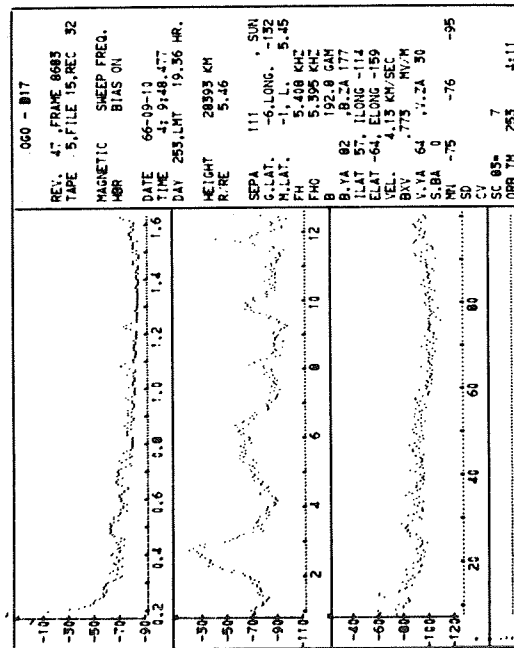
kHz OGO-3

10 SEPT 66

0410:00 UT



0409:48 UT



0410:47 UT

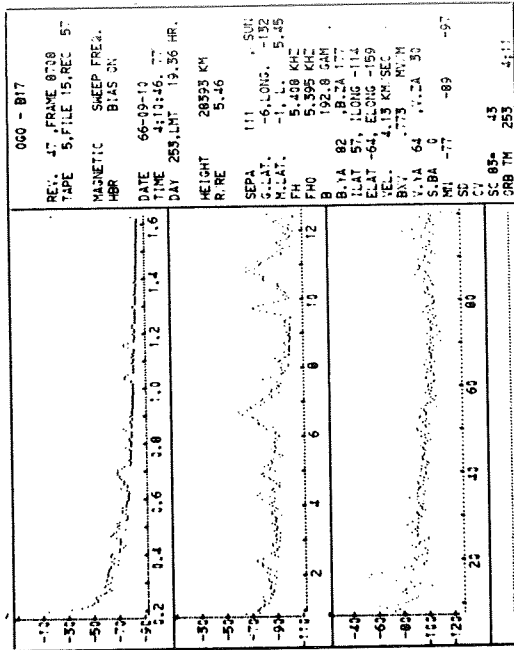


FIGURE 18. Unusual narrowband radiation above the local (Williams-Mead) electron gyrofrequency  $f_H = 5.4$  kHz. The broadband spectrogram shows several radiation bands both above and below  $f_H$  (the diagonal lines above the 13 kHz nominal receiver cutoff are interference). Two frames of digital data from slightly different times show amplitude (dbv) vs. frequency (kHz) for the three OGO-3 sweeping receivers. Several bands of radiation can be seen including one at about 16 kHz on the second frame.

narrowband activity at 6.8 , 10.9 , and 16 kHz . The 16 kHz noise has a field strength of nearly 10 milligammas (over the 600 Hz filter bandwidth) and its frequency is approximately three times the expected gyrofrequency of 5.4 kHz .

Concurrent ground data from Byrd and Great Whale stations ( $L \sim 7$ ) at nearly the same meridian as the satellite show marked substorm activity (planetary 3-hour  $K_p = 4^+$ ). Auroral VLF hiss is seen intermittently at Byrd from about 0000 until 0413 UT; it is strongest at about 0406. There are auroral breakups, as evidenced by sudden large ULF micropulsation and 5577 Å all sky photometer increases, at 0334 and again at 0413 at both stations. Byrd sees a final breakup at 0419, the same time noise above the gyrofrequency ceases at the satellite. Magnetic activity is comparatively low at both stations the remainder of the night. While it is not certain that this substorm activity is related to the radiation above the gyrofrequency at the equator, the fact that the radiation ceases upon the final auroral breakup of the evening is enticing.

Nose whistlers are received at Byrd throughout the period 0350 - 0440 UT. The nose frequency of the strong trace believed to be propagating just outside the plasmopause increases from slightly over 4 kHz to slightly over 5 kHz , although the poorly-defined leading edge makes measurement inexact. This would indicate an inward movement of the plasmopause from about  $R_o = 4.6$  to  $R_o = 4.3$  . The equatorial electron density at this distance can be estimated by measuring the time delay between the causative spheric and the whistler at the nose frequency. The 1.2 second time delay indicates an electron density of about

$32 \text{ cm}^{-3}$ , or a plasma frequency of 51 kHz. Further out at the OGO-3 position the density can be crudely estimated by assuming an  $R^{-4}$  distribution of electrons. At  $R_0 = 5.5$  the plasma frequency would then be about 31 kHz, considerably above the highest frequency radiation observed.

Little theoretical analysis of this event has been undertaken; however, two possibilities come to mind. First, the noise may in fact be above the local electron gyrofrequency in which case it would not propagate in the whistler mode. For example thermal plasmas may exhibit electrostatic instabilities at frequencies near multiples of the electron gyrofrequency [Stix, 1962]. Second, and probably less likely, a very large particle flux might increase the local magnetic field strength so the noise was actually below the electron gyrofrequency. In any case temporary dynamic particle fluxes might be expected from the substorm activity on the ground.

### III. SUGGESTIONS FOR FURTHER RESEARCH

Many avenues of fruitful research into banded chorus now seem possible. In addition to the banded chorus frequency, the slopes of the emissions should be scaled and studied statistically--consequences of the generation theory of Helliwell [1967], for example, are that falling tones should not be observed at the equator, rising tones should be about twice as common at the equator as at high latitudes, and in general the slope of an emission should be proportional to the distance from the equator to the generation region. Banded chorus amplitudes, determined from the OGO-1 VCO or the digital data from either OGO 1 or OGO 3, should also be routinely scaled and studied; both as a function of latitude or fieldline distance from the equatorial generation region to determine the amount of attenuation; and as a function of  $L$  and local time to determine the average energy of banded chorus activity in different regions of the magnetosphere.

Detailed spectral analysis of individual emissions could provide valuable insight into the generation mechanism. The continuous frequency spectrum of the OGO broadband data and the 3 msec time response of the OGO-1 amplitude VCO permit detailed measurements of such parameters as rise time, decay time, bandwidth, and the variation of frequency, amplitude, and bandwidth with time. Correlation of banded chorus with OGO low energy (1-50 keV) electron measurements, both statistically and in case studies, would also be highly interesting.

Study of the average variation of the normalized frequency  $f/f_{Ho}$  has suggested that banded chorus is nonducted and in general deviates to lower  $L$ -values as it propagates earthward. Detailed study of the variation of normalized frequency for particular passes might lead to the identification

of ducts (c.f. ground whistler data), electron density gradients (c.f. OGO mass spectrometer data), and magnetic field distortions (c.f. OGO magnetometer data) in the plasma trough.

Present understanding of the relation of ground observed chorus to banded chorus is quite limited. A wealth of OGO-2 and OGO-4 data are available for this sort of study, although observations at higher altitudes (e.g. 6000 km,  $55^{\circ}$  magnetic latitude) would be useful. Efforts to match ground emissions to satellite emissions should be continued--simple ground VLF receivers at the satellite tracking stations would be particularly helpful for this purpose.

## REFERENCES

- Angerami, J. J. and D. L. Carpenter, Whistler studies of the plasmopause in the magnetosphere, 2, electron density and total tube content near the knee in magnetospheric ionization, J. Geophys. Res., 71, 711, 1966.
- Barrington, R. E., J. S. Belrose and D. A. Keeley, Very-low-frequency noise bands observed by the Alouette 1 satellite, J. Geophys. Res., 68, 6539, 1963.
- Bell, T. F. and O. Buneman, Plasma instability in the whistler mode caused by a gyrating electron stream, Phys. Rev., 133, A1300, 1964.
- Brice, N. M., An explanation of triggered VLF emissions, J. Geophys. Res., 68, 4626, 1963.
- Brice, N. M., Fundamentals of very low frequency emission generation mechanisms, J. Geophys. Res., 69, 4515, 1964.
- Brice, N. M., Bulk motion of the magnetosphere, J. Geophys. Res., 72, 5193, 1967.
- Burtis, W. J. and R. A. Helliwell, Banded chorus--a new type of VLF radiation observed in the magnetosphere by OGO 1 and OGO 3, J. Geophys. Res., 74, 3002, 1969.
- Carpenter, D. L., Whistler studies of the plasmopause in the magnetosphere, 1, temporal variations in the position of the knee and some evidence on plasma motions near the knee, J. Geophys. Res., 71, 693, 1966.
- Dowden, R. L., Doppler-shifted cyclotron radiation from electrons: a theory of very low frequency emissions from the exosphere, J. Geophys. Res., 67, 1745, 1962.
- Dunckel, N. and R. A. Helliwell, Whistler-mode emissions on the OGO-1 satellite, J. Geophys. Res., (in press) 1969.
- Ficklin, B. P., L. H. Rorden, R. A. Helliwell and N. Dunckel, Two new low-frequency noise phenomena observed on OGO 1, (in preparation) 1969.
- Gallet, R. M., The very low frequency emissions generated in the earth's exosphere, Proc. IRE, 47, 211, 1959.
- Gurnett, D. A. and B. J. O'Brien, High-latitude geophysical studies with satellite Injun 3, 5, very-low-frequency electromagnetic radiation, J. Geophys. Res., 69, 65, 1964.
- Helliwell, R. A., Whistlers and Related Ionospheric Phenomena, Stanford University Press, Stanford, Calif., 1965.
- Helliwell, R. A., A theory of discrete VLF emissions from the magnetosphere, J. Geophys. Res., 72, 4773, 1967.

- Jelly, D. and N. Brice, Changes in Van Allen radiation associated with polar substorms, J. Geophys. Res., 72, 5919, 1967.
- Kavanagh, L. D., Jr., J. W. Freeman, Jr. and A. J. Chen, Plasma flow in the magnetosphere, J. Geophys. Res., 73, 5511, 1968.
- Kennel, C. F. and H. E. Petschek, A limit on stably trapped particle fluxes, J. Geophys. Res., 71, 1, 1966.
- Laaspere, T., M. G. Morgan and W. C. Johnson, Chorus, hiss and other audio-frequency emissions at stations of the Whistlers-East network, Proc. IEEE, 52, 1331, 1964.
- Lee, B. G., Spectrum analysis of VLF emissions, Tech. Rept. SU-SEL-68-081, Radioscience Lab., Stanford Electronic Labs., Stanford University, Stanford, Calif., August 1968.
- Lincoln, J. V., Geomagnetic and solar data, J. Geophys. Res., 72, 1967.
- Oliven, M. N. and D. A. Gurnett, Microburst phenomena, 3, an association between microbursts and VLF chorus, J. Geophys. Res., 73, 2355, 1968.
- Pope, J. H., A high-latitude investigation of the natural very-low-frequency electromagnetic radiation known as chorus, J. Geophys. Res., 68, 83, 1963.
- Rorden, L. H., L. E. Orsak, B. P. Ficklin, and R. H. Stehle, Instruments for the Stanford University/Stanford Research Institute VLF experiment (4917) on the EOGO satellite, Stanford Research Institute Report, Menlo Park, Calif., May 1966.
- Russell, C. T., R. E. Holzer, and E. J. Smith, OGO-3 observations of ELF noise in the magnetosphere, 1, spatial extent and frequency of occurrence, J. Geophys. Res., 74, 755, 1969.
- Stepanov, K. N. and A. B. Kitsenko, Excitation of electromagnetic waves in a magnetoactive plasma by a beam of charged particles, Sov. Phys.-Tech. Phys., 6, 120, 1961.
- Stix, T. H., The Theory of Plasma Waves, McGraw-Hill Book Co., New York, 1962.
- Taylor, W. W. L. and D. A. Gurnett, Morphology of VLF emissions observed with the Injun-3 satellite, J. Geophys. Res., 73, 5615, 1968.
- Thorne, R. M. and C. F. Kennel, Quasi-trapped VLF propagation in the outer magnetosphere, J. Geophys. Res., 72, 857, 1967.
- Ungstrup, E. and I. M. Juckerott, Observations of chorus below 1500 cycles per second at Godhavn, Greenland, from July 1957 to December 1961, J. Geophys. Res., 68, 2141, 1963.



Vasyliunas, V. M., Low-energy electrons on the day side of the magnetosphere (letter), J. Geophys. Res., 73, 7519, 1968.

Venkatesan, D., M. N. Oliven, P. J. Edwards, K. G. McCracken and M. Steinbock, Microburst phenomena, 1, auroral zone X-rays, J. Geophys. Res., 73, 2333, 1968.

Williams, D. J. and G. D. Mead, Nightside magnetosphere configuration as obtained from trapped electrons at 1100 kilometers, J. Geophys. Res., 70, 3017, 1965.